Recent progress on the use of lignin-based porous carbon in supercapacitors

ZHA Ding-chen[1,†], WANG Jia-heng[1,†], Hao Rui-xiang[2], Wu Yun-feng[2], LI Xiu-he[2], ZHAO Jia-wen[3], LI Wen[1], PIAO Wen-xiang[1,2,*], JIANG Nan-zhe[1,2,3,*]

(1. *Department of Polymer Materials and Engineering*, *College of Engineering*, *Yanbian University*, *Yanji* 133002, *China*;
2. *Department of Materials and Chemical Engineering*, *College of Engineering*, *Yanbian University*, *Yanji* 133002, *China*;
3. *Department of Chemistry*, *College of Science*, *Yanbian University*, *Yanji* 133002, *China*)

Abstract: With the development of electronics and portable devices, there is a significant drive to develop electrode materials for supercapacitors that are lightweight, economical, and provide high energy and power densities. Lignin-based porous carbons have recently been extensively studied for energy storage applications because of their characteristics of large specific surface area, easy doping, and high conductivity. Significant progress in the synthesis of porous carbons derived from lignin, using different strategies for their preparation and modification with heteroatoms, metal oxides, metal sulfides, and conductive polymers is considered and their electrochemical performances and ion storage mechanisms are discussed. Considerable focus is directed towards the challenges encountered in using lignin-based porous carbons and the ways to optimize specific capacity and energy density for supercapacitor applications. Finally, the limitations of existing technologies and research directions for improving the performance of lignin-based carbons are discussed.

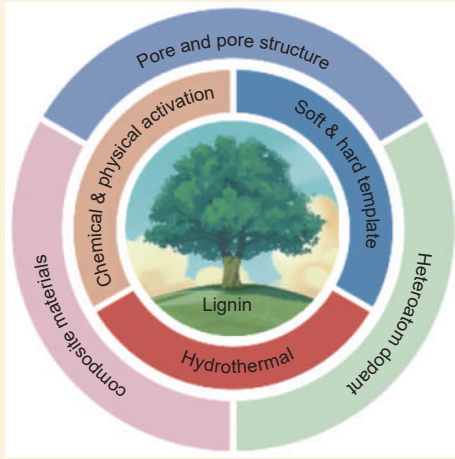

Key words: Lignin；Porous carbon；Supercapacitor；Carbonization

1 Introduction

With the development of the economy, the global energy demand has been increasing. But the heavy use of fossil fuels has led to depletion of energy resources and destruction of the atmosphere, which is why, to fix' this, the most critical strategy is to reduce fossil fuel consumption and develop renewable energy. So, new clean energy sources such as solar, wind, and tidal power have been emerging rapidly, and efficient energy storage has also become a hot topic recently. This is because most clean energy generation is intermittent, so the energy storage device needs to balance fluctuations. In addition, development of electric vehicles has further intensified the research efforts on energy storage devices. As a result, new electrochemical energy storage devices (e.g., supercapacitors[1–2] , alkali metal-ion batteries[3–5] , metal-air battery[6–7] etc.) have attracted much attention because of their advantages of high performance, low cost, long service life and good safety, and have been utilized in various fields such as portable electronic devices and electric vehicles. Supercapacitor is an electrochemical capacitor that has high power density, large capacity and that does not decay significantly even after millions of cycles[8–9]. It stores and releases energy by reversible desorption and adsorption of ions at the electrode-electrolyte interface.

Supercapacitors can be mainly divided into 3 categories based on their energy storage mechanisms (Fig. 1): (1) Electric double layer capacitors (EDLC) store energy through electrostatic adsorption in the in-

Received October 10, 2024
Revised December 23, 2024
Accepted December 23, 2024

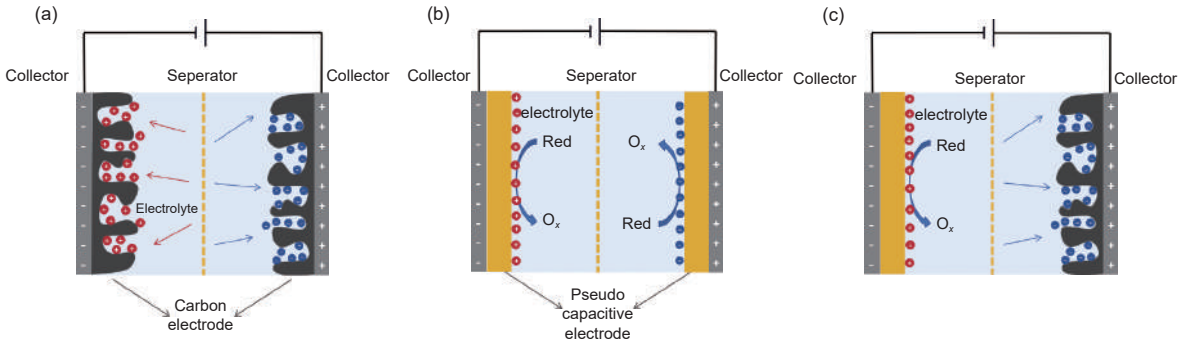

Fig. 1 Structure of (a) EDLC, (b) PC and (c) HSC

terface between electrodes and electrolyte. (2) Pseudocapacitors (PC) store energy through a rapid redox reaction on the surface of metal oxides or conductive polymers. (3) Hybrid supercapacitors (HSC), which currently are the mainstream of commercial supercapacitors. The most important thing for supercapacitor is the choice of electrode material, which influence their capacitance, energy density and other crucial attributes. So the development of superior electrode materials is an important aspect in preparing high-performance supercapacitors. Based on this background, a variety of electrode materials have been developed, especially porous carbon, which have received increased attention due to their excellent supercapacitive properties.

Various porous carbon materials, such as activated carbon powder, activated carbon fiber, carbon gel, carbon nanotubes, have been reported to be used as supercapacitor electrode materials[10–12]. Porous carbon, with high specific surface area and diverse structures, is the most popular research direction in the field of supercapacitors[13]. Porous carbon is generally manufactured by high-temperature carbonization of organic precursors such as biomass[14]. Lignin, with a carbon content of more than 60%, is a very promising carbon precursor in biomass[15].

Lignin is the second most abundant naturally polymer, accounting for about 30% of the biosphere's organic carbon and it is the only renewable raw material composed of aromatic monomers[16]. The major structural units of lignin are H (p-hydroxyphenyl), G (guaiacyl) and S (syringyl). These units are linked by various C—O and C—C bonds, such as the illustrated β-O-4, α-O-4, 4-O-5, 5-5, β-β, β-5, and β-1 bonds (Fig. 2). The content of each structural unit varies based on the origin of the lignin, mainly softwoods, hardwoods and grasses. The composition and structure of lignin in plants vary according to species, site and growth period and even the natural environment[18–19]. Therefore, there are differences in the pyrolysis characteristics of lignin from different sources. Generally, the thermal stability of hardwood lignin is weaker than that of softwood lignin. This is because ether bonds between S—S units are more prone to breakage compared to those between G—G units[20] (Table 1), hardwood lignin contains more S units. Additionally, hardwood lignin has a higher content of β-O-4 bonds, which exhibit weaker thermal stability, while the content of 5-5 bonds, which have stronger thermal stability, is lower than that in softwood lignin.

The structure of lignin is significantly impacted by different production methods. Björkman lignin, recognized as the closest to natural lignin in structure, retains —O— bonds well and thus exhibits high reactivity[21], making it primarily used in chemical research. For lignin produced industrially, it mainly originates from wood hydrolysis industry and paper industry. The wood hydrolysis industry yields Klason lignin and Wilstatter lignin. The acid and alkaline pulping processes in traditional paper industry produce kraft lignin and alkali lignin, respectively, while novel pulping techniques using organic solvents can obtain organosolv lignin. Compared to Björkman lignin, alkali lignin undergoes hydrolysis of linking bonds such as —O— bonds, accompanied by oxida-

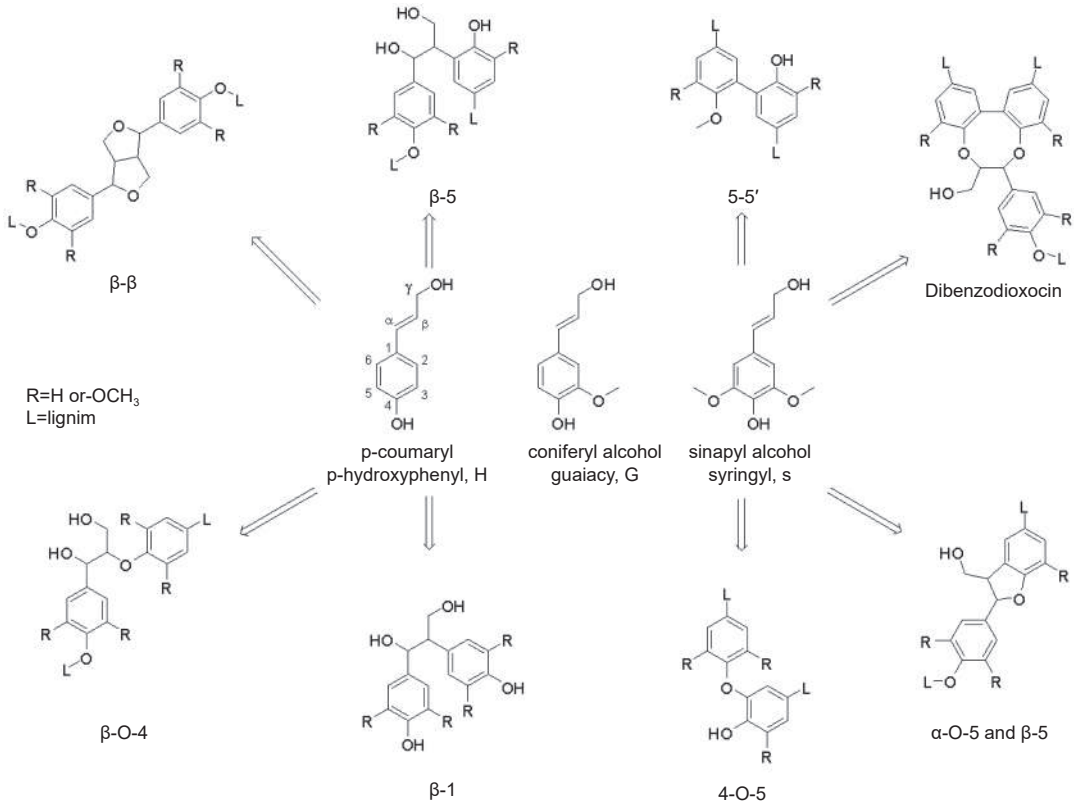

Fig. 2 Major structural units of lignin and their connections. Adapted with permission from ref.[17]. Copyright 2012, Elsevier

Table 1 Mount of the different monolignols in lignin from various plant types

Plant types	H/%	G/%	S/%
Softwoods	<5	>95	0
Hardwoods	0-8	25-50	45-75
Grasses	5–35	35–80	20–55

tion reactions, resulting in higher contents of —OH and —COOH groups on the side chains and more C=O groups on the aromatic rings[22]. During the extraction process of Klason lignin, strong condensation reactions occur, and $-OCH_3$ groups are removed during sulfuric acid treatment[23]. Adding sulfuric acid to organosolv lignin leads to the cleavage of α and β ether linkages and the dehydration of alcoholic hydroxyl groups[24].

The pyrolysis behavior of lignin also varies significantly depending on the method of lignin preparation. For example, Chen et al.[25] compared the pyrolysis of Klason lignin extracted from herbaceous biomass with that of commercial alkali lignin and found that alkali lignin contains more G units than Klason lignin. Wang et al.[26] prepared four common types of lignin from pine wood as raw material and studied their structural characteristics and pyrolysis properties. They found that the less stable ether bonds and side chains were well-protected in alkali lignin and Björkman lignin, which resulted in a lower temperature requirement for initial pyrolysis and the production of more phenolic compounds. The weight percentage of the final residues for the four samples were: Björkman lignin < organosolv lignin < alkali lignin < Klason lignin. The final residue weight increased with decreasing in the $-CH_3$ content, indicating that lignin with lower $-CH_3$ content had better stability and denser structural units, leading to the production of more char.

Due to the high degree of aromatization of lignin, lignin-based carbon has a higher graphitization degree, higher yield, and greater potential for application in electrochemical energy storage devices. While

it offers supercapacitors high power density and superior cycle life, its low capacitance and energy density are significant drawbacks that restrict the application of supercapacitors. Consequently, a variety of optimization strategies have been proposed recently to boost the capacitance performance of supercapacitors. These strategies encompass refining the synthesis process, adjusting the pore structure, doping heteroatoms to improve capacitance, and developing composite materials based on carbon. As it contains —OH, —C=O, —O—C, —COOH and other functional groups, which could be subject to various modification reactions, lignin has great potential application value as a dopant.

The aim of this review is to provide a comprehensive and up-to-date analysis of the research progress in lignin-based porous carbon in recent years, with a particular focus on its application in supercapacitors. This review distinguishes itself by offering a more holistic and critical examination of the field, integrating the latest advancements and emerging trends. We meticulously describe and compare various preparation methods of lignin-based porous carbon, emphasizing novel techniques and their impact on material properties. The review goes beyond mere summarization by critically evaluating different methods to improve supercapacitor performance, including innovative approaches to pore structure engineering, cutting-edge heteroatom doping strategies, and state-of-the-art composite formations of lignin-based porous carbon materials. Additionally, we provide an in-depth analysis of the synergistic effects between these methods, offering insights not typically covered in existing literature. The review also stands out by presenting a forward-looking perspective on the challenges and future development directions of supercapacitors based on lignin-derived porous carbon electrodes.

2 Synthesis methods of lignin-based porous carbon

The pyrolysis of lignin can be generally divided into 3 stages: (1) Thermal evaporation of free water; (2) Removal of thermally unstable structures on the chains of the lignin macromolecular structure, including the breakage of ether bonds between structural units and the partial pyrolysis of structural units; (3) Evolution of the aromatic ring of lignin to a fused ring structure and eventually to a carbon matrix[27–28].

2.1 Activation

2.1.1 Physical activation

Usually, physical activation can be divided into two steps: carbonization and activation. Carbonization refers to placing carbon precursors in an oxygen free atmosphere and heating them at a certain temperature (200–400 °C). During the carbonization process, C atoms spontaneously rearrange with increasing temperature and form a graphite microcrystalline structure. At the same time, small molecules evaporate to form narrow primary pores, making the ultimate product structure is more orderly and beneficial for improving the conductivity of carbon[29]. During the activation process, the N_2 (H_2O or CO_2) in the atmosphere acts as an activator, which undergoes oxidation-reduction reactions with amorphous carbon or heteroatoms to deepen the primary pores, expose the surface of microcrystals, and gradually form interconnected pores[30–31]. Due to the reaction activity of C atoms, the reaction rates in each direction vary, resulting in the formation of interconnected hierarchical porous network structures, so during the preparation process, the structural composition of the final carbon material can be controlled by adjusting parameters such as activation temperature, activation time, and gas flow rate. CO_2 and H_2O (vapor) have become the most commonly used activators in the industrial production for activated carbon due to their simple process and low cost. Focusing on water vapor as an example, the interaction between H_2O and carbon typically takes place at elevated temperatures, resulting in the formation of CO_2 or CO. Subsequently, CO_2 can react further with carbon, leading to the etching of the carbon and the creation of pores[9].

$$C + H_2O \rightarrow H_2 + CO$$

$$C + 2H_2O \rightarrow 2H_2 + CO_2$$

$$CO_2 + C \rightarrow 2CO$$

$$2CO + O_2 \rightarrow 2CO_2$$

As shown in Table 2, during the carbonization process, the carbonization temperature had a significant effect on the structural parameters of the lignin-based porous carbon, and with the increase of the carbonization temperature, the specific surface area and microporous volume of the carbon showed a tendency of increasing first and then decreasing. At temperatures between 250 and 450 °C, there was a significant increase in both parameters. From 450 °C, the values of specific surface area and microporous volume no longer increased with the increase of temperature, which indicated that the carbon material had formed a relatively stable structure when the carbonization temperature reached 450 °C[32]. In addition, beyond 450 °C, the change in pore volume was not obvious, indicating that the organic matter is decomposed relatively sufficiently. But there is a decrease in the specific surface area of LPC carbonized at 500 °C to 600 °C. The same phenomenon occurred when the activation temperature was too high. This may attribute to high temperatures collapse part of the pores in carbon framework.

As shown in Table 2, the volume of micropores increased as the pyrolysis time was extended from 90 to 180 min. When the pyrolysis time exceeds 120 min, the specific surface area of the carbon material decreases with the extension of time, which is due to the activation reaction involving more aromatic carbon atoms, resulting in the overconsumption of a limited number of carbon atoms in the active sites[33]. Further etching of the carbon skeleton results in a decrease in the specific surface area. The specific surface area of carbon materials activated by H_2O is higher than that of carbon materials activated by CO_2. This is because CO_2 is not that active in generation of pores in the lignin-derived carbon[35]. And H_2O plays an important role in mesoporous formation. Jiang et al.[36] found the competitive adsorption of CO_2 and H_2O on the carbon surface leads to a small synergistic effect of pore formation. The effect of CO_2 on the formation of pores is poor, and the pores are mainly micro-pores, which is due to the lower activity for deoxygenation.

In summary, physical activation methods offer advantages such as high carbon yield, low corrosion to equipment, and easy control of the activation degree. However, the carbon prepared through these methods mainly consist of micropores, with a narrow pore size range, underdeveloped pore structure, and low specific surface area. These drawbacks significantly impact their performance as electrodes for supercapacitors.

2.1.2 Chemical activation

The chemical activation method involves mixing the carbon precursor with an activator and then heat-treating the carbon precursor in the temperature range of 400–900 °C. Unlike physical activation, chemical

Table 2 The parameter comparison of lignin-based porous carbon prepared by physical activation

Materials	Preparation method	Carbonization temperature/°C	Activation temperature/°C	Activation duration/min	Specific surface area/ ($m^2\ g^{-1}$)	Micropore volume/ ($cm^3\ g^{-1}$)	Ref.
Black liquor lignin	H_2O	250	800	40	86.4	0.02	[32]
		350			142.2	0.04	
		450			288.8	0.08	
		550			242.9	0.06	
Hydrolysis lignin	H_2O	—	800	30	506.0	0.22	[33]
				60	492.0	0.21	
				120	616.0	0.26	
Lignin/PEG99/1	H_2O	250	900	60	854.0	0.43	[34]
Alkali lignin	CO_2	750	750	30	460.0	0.14	[35]
	H_2O				79.0	0.03	
Dealkalized lignin	N_2	500	800	60	474.0	0.16 (80%)	[36]
	CO_2				516.1	0.17 (74%)	
	H_2O				804.1	0.20 (54%)	
	CO_2+H_2O				674.8	0.18 (57%)	

activation is usually done in single carbonization step. The activators used for chemical activation are KOH, NaOH, K_2CO_3, $ZnCl_2$ and H_3PO_4, among which KOH, $ZnCl_2$ and H_3PO_4 are the most commonly used activators[37–39].

The KOH activator is widely utilized primarily due to the high specific surface area (SSA) and pore volume that the resulting carbon material possesses. Currently, it is believed that the reaction mechanism of KOH in pore formation within porous carbon mainly includes the following four steps: (1) KOH reacts with carbon to generate potassium compounds such as K_2CO_3 and K_2O. (2) Further reaction occurs between carbon and K compounds (KOH, K_2O and K_2CO_3) by continuing to elevate the temperature, and K compounds etch the carbon matrix to form a pore network and ultimately generate K metal. (3) The by-products H_2O, H_2, CO and CO_2 will further react with carbon to promote the development of pores. (4) The metal K produced in the reaction will be inserted into the carbon lattice, which will cause the expansion of the pores, and when the metal K is cleaned up by the acid at a later stage, it will leave the microporous structure. The relevant reactions are as follows:

$$6KOH + 2C \rightarrow 2K + 3H_2 + 2K_2CO_3$$

$$K_2CO_3 + 2C \rightarrow 2K + 3CO$$

$$K_2CO_3 \rightarrow K_2O + CO_2$$

$$2K_2O + C \rightarrow 4K + CO_2$$

$$K_2O + C \rightarrow 2K + CO$$

In chemical activation, pre-carbonization can also serve as an effective method to boost the SSA and porosity of carbon[40–42], especially in improving the microporous volume, and the carbonization temperature has a significant effect on the structural parameters such as the SSA and the pore volume of lignin-based porous carbon[40]. By enlarging the lignin-activator ratio, the SSA and microporous capacity of the carbon material can be increased, and the mesopore percentage will also be increased[41–43]. Excessive activator and excessive time will destroy the carbon framwork, which will lead to the collapse of the interconnected carbon walls, resulting in a decreasing trend of specific surface area and pore volume[41–42].

Different from the activation mechanism of KOH, $ZnCl_2$ mainly plays a role of dehydration in the activation process. There is evidence suggesting that condensation reactions of aromatics, for example, alkylation and acetylation reactions, are more likely to occur in the presence of Zn compounds[44]. So $ZnCl_2$ is able to promote pyrolysis and aromatization of the material, forming a porous structure and inhibiting the generation of most monomer phenols and tars[45–46]. As shown in Table 3, the highest SSA and pore volume of the lignin-based porous carbon prepared by $ZnCl_2$ activation was relatively low compared with that of KOH activation[47–48], which was attributed to the

Table 3 The parameter comparison of lignin-based porous carbon prepared by chemical activation

Materials	Activating agent	Weight ratio (w lignin/w Activation agent)	Carbonization temperature/°C	Activation temperature/°C	Specific surface area/($m^2\ g^{-1}$)	Pore volume/($cm^3\ g^{-1}$)		Ref.
						Micropore	Mesopore	
Lignin-rich residue	KOH	1 : 3	450	700	3004	1.57 (total)		[40]
Black liquor lignin	KOH	1 : 2	—	800	1337	0.53	0.04	[47]
	$ZnCl_2$				896	0.32	0.04	
Alkali lignin	N_2	1 : 1	—	700	116	0.01	—	[48]
	$ZnCl_2$				866	0.30		
	KOH				1191	0.42		
	K_2CO_3				1585	0.59		
Alkali lignin	KOH	1 : 3	400	800	2859	0.70	0.91	[41]
Kraft lignin	K_2FeO_4	1 : 1	180	800	752	0.38 (total)		[49]
		1 : 2			2352	1.44 (total)		
		1 : 3			1100	0.64 (total)		
Hydrotropic lignin	H_3PO_4	1 : 2	200	450	2015	0.19	0.73	[42]
		1 : 1		500	1321	0.51	0.08	
		1 : 3		500	1790	0.16	1.13	
Lignin	H_3PO_4	—	—	600	98.28	0.09 (total)		[51]

weaker etching effect of $ZnCl_2$ on carbon. What's worth mention, although $ZnCl_2$ is highly effective in activation, $ZnCl_2$ is much more harmful to human health than other activation agents, and it can easily pollute water during preparation, storage, and usage process. This discrepancy with the concept of green chemistry has led to the eventual replacement of $ZnCl_2$ by H_3PO_4 in industrial production.

The mechanism of activation of H_3PO_4 has not been fully understood. One possible mechanism is shown in Fig. 3. H_3PO_4 is an acidic catalyst that promotes processes such as cyclization, condensation and facilitates bond cleavage to form cross-links and binds to organic matter to form phosphates and polyphosphates that link and cross-link biopolymer fragments, the inserted phosphate group promotes swelling to occur and upon removal of the acid, the char base retains the pore structure in the swollen state. As can be seen from Table 3, the porous carbon obtained with H_3PO_4 has more mesopores and the activation temperature is lower than that of KOH and $ZnCl_2$[50–51].

Compared to physical activation, chemical activation offers the following advantages: (1) The prepared carbon materials possess a larger SSA and well-developed pore structure. (2) The activation process requires a shorter duration. (3) Carbonization and activation occur simultaneously, simplifying the preparation process. (4) Different activating agents can create pores of varying sizes, for instance, $ZnCl_2$ produces porous carbon with developed micropores and mesopores, H_3PO_4 activated carbon with developed mesopores, and KOH activated carbon with developed micropores. These benefits allow porous carbon prepared through chemical activation to display superior electrochemical properties when employed as electrode materials in supercapacitors. However, the chemical activation process may produce harmful gases that pollute the environment, and the chemical activating agents can be corrosive to equipment. This has emerged as a pressing technical challenge in the domain of porous carbon fabrication that requires immediate attention from researchers.

2.2 Template

2.2.1 Soft template

The soft template method, also known as the organic template method, involves combining a polymeric soft template with a precursor to create a structured mesoporous precursor. Then, through high-temperature treatment, the template is removed, thereby forming porous carbon. Specifically speaking, the soft

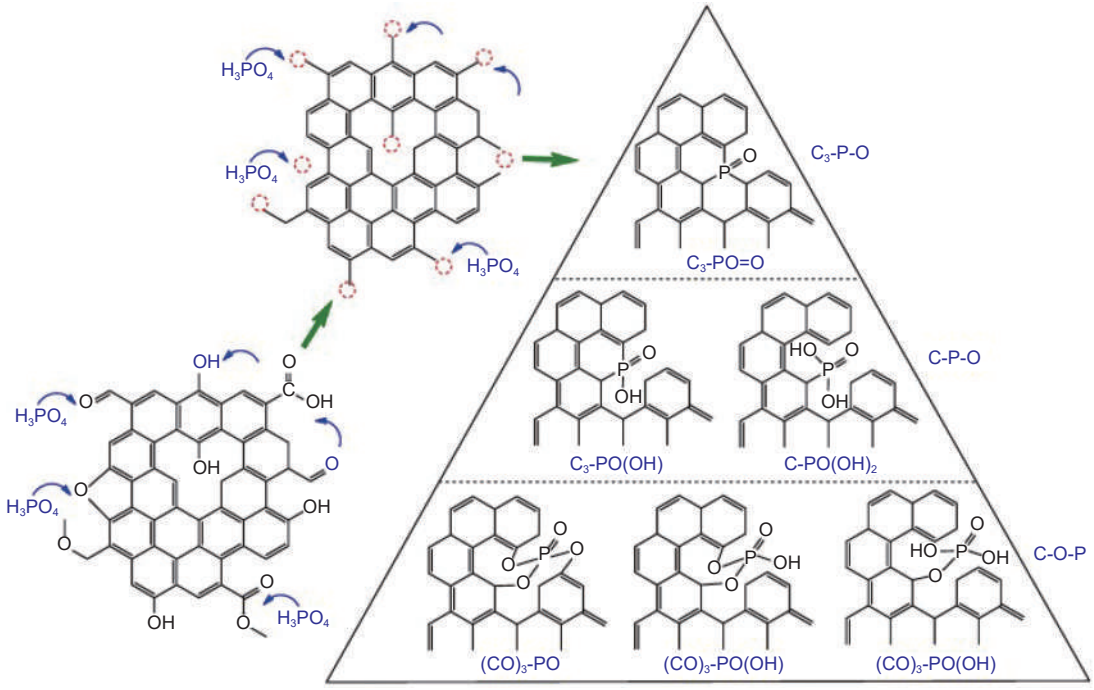

Fig. 3 Possible chemical reaction pathways of H_3PO_4 activation during biomass pyrolysis. Adapted with permission from ref.[52]. Copyright 2022, Elsevier

template and lignin molecules in the solvent environment self-assemble to forming composite nanomicelles by electrostatic or hydrogen bonding, carbon chain of the soft template decomposed during carbonization to form pore channels in the lignin matrix. Commonly used soft template agents include F127, CTAB and P123, among which F127 triblock copolymer is the most widely used.

The soft template method does not need to remove the template after carbonization and has the advantages of simple preparation and low cost. However, carbon materials prepared by the soft template method are predominantly mesoporous and have a low specific surface area. To solve this problem, researchers have made numerous attempts in recent years, among which the most widely used approach is dual-template[53], the coupling of soft templates with hard templates. This method significantly increases the SSA and pore volume of the soft-templated carbon. During the process, hard templates serve as scaffolds to preserve the integrity of the desired pore structure against degradation from high-temperature. Concurrently, the soft template predominantly dictates the development of mesopores[54].

In the dual-template method, the soft template agent not only plays the role of pore creation, but also disperses the hard template agent to prevent agglomeration in the lignin matrix. Wu et al.[55] used SiO_2 and F127 to prepare mesoporous carbon with enhanced specific surface area and pore volume, it is worth mentioning that the calcium lignosulfonate has better effects than the sodium lignosulfonate in the formation of the pore structure, which is due to the stronger coordination between Ca^{2+} and hydroxyl groups of F127 than Na^{+}[56] , resulting in better binding of F127 to calcium lignosulfonate during solvent evaporation. Song et al.[57] used alkali lignin, MgO and F127 to prepare mesoporous carbon with a SSA of 712 $m^2\ g^{-1}$ and total pore volume of 0.90 $cm^3\ g^{-1}$, respectively, mesoporous content of more than 83%. In the carbonization process, MgO nanoparticles acted as a main template by occupying the space, whereas F127 acted as a dispersant and soft template for preventing the agglomeration of MgO. The resulting carbon has a high specific capacitance of 186.3 F g^{-1} when used as supercapacitor electrodes.

The interaction between the soft templating agent and the lignin influences the ordered structure of the porous carbon, so the type of soft templating agent and its concentration are key factors affecting the structural parameters of the resulting lignin-based porous carbon (Fig. 4)[58]. Soe et al.[59] used polymethylmethacrylate (PMMA) as templating agent and lignin as precursor to produce foam carbon. They tested three different PMMA contents (100%, 200% and 300%), producing foam carbon samples with respective bulk densities of 0.58, 0.41, and 0.39 g cm^{-3} and with porosities of 71.2%, 79.5% and 80.5%. This study reveals that the level of porosity primarily depends on the amount of template used. Specifically, when the PMMA template content exceeds 200%, it leads to polymerization and precipitation. This causes a loss of solution homogeneity before gelation, resulting in an inhomogeneous pore space in the final product. Moreover, the excess organic template releases a significant volume of volatile compounds during carbonization, which can compromise the structural integrity of the framework of carbon. The soft template method for producing lignin-based porous carbon is significantly influenced by the molecular weight of lignin, which plays a crucial role in determining the pore structure of these carbon, Qin et al.[60] prepared ordered mesoporous carbon using F127 and lignin with different molecular weights, in which the lignin with the smallest molecular weight (1055 g mol^{-1}) had the largest SSA (466.1 $m^2\ g^{-1}$) , highest pore volume (0.62 $cm^3\ g^{-1}$) and clearer mesoporous channels. This suggests that as molecular weights increase, the integrity of the nanomicelle structure is compromised.

2.2.2 Hard template

The hard template method generally uses inorganic materials with specific structure and morphology, which fills the pores of the templates with carbon precursors, and then converts them into target products by high-temperature treatment, and finally

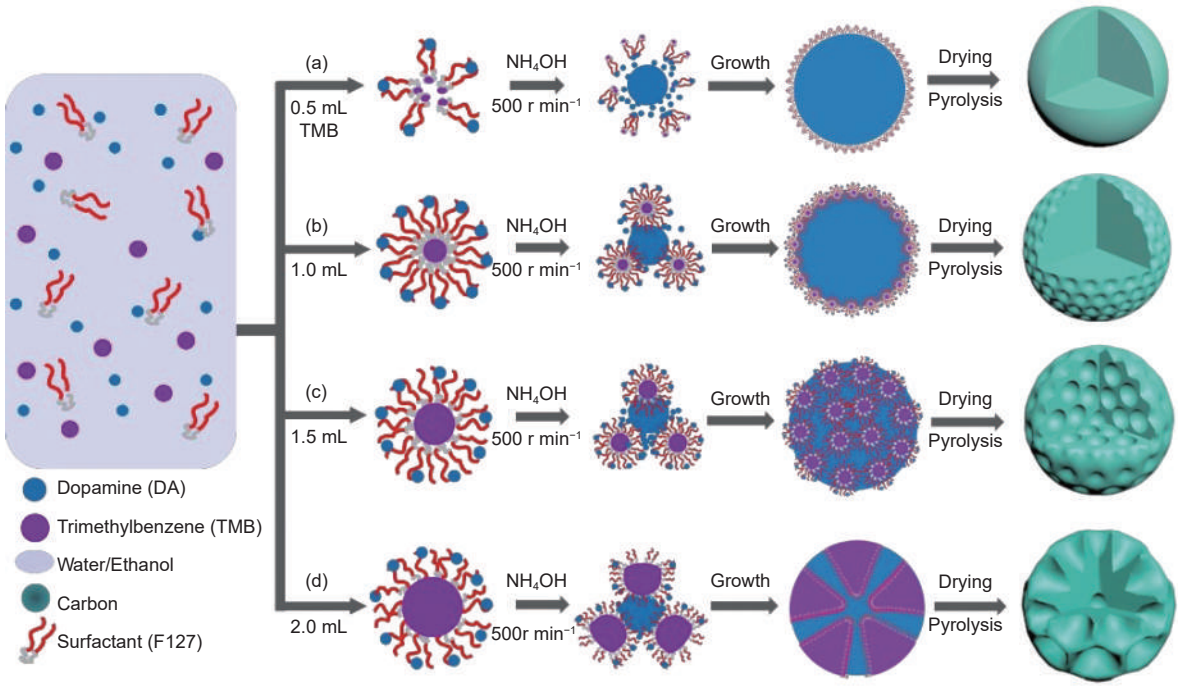

Fig. 4 Schematic diagram of the process for preparing mesoporous carbon nanospheres with different morphologies and structures using the nano-emulsion assembly method. Adapted with permission from ref.[58]. Copyright 2019, American Chemical Society

removes the templates to obtain porous carbon[61]. In comparison to the soft template method, the hard template method can more accurately regulate the pore size distribution and morphology of porous carbon by adjusting the template. As such, the particle size and dispersion of the hard template agent play a significant role in determining the pore size distribution of lignin-based porous carbon. The resulting porous carbon obtained through the hard template method exhibits high SSA and ordered pore structure.

However, the traditional hard template are silica-based templates, including nano SiO_2 spheres and zeolites[62], which require the use of HF, NaOH or KOH to be removed. The use of these reagents not only complicates the preparation process but also adds time and financial expenses. Therefore, researchers have developed many new types of green templates, including salts such as $CaCl_2$, NaCl and KCl, as well as metal oxides such as CaO, ZnO and MgO. Zhang et al. synthesized a lignin-based flower-like carbon with ZnO as a template (Fig. 5). Wang et al.[64] used nano MgO produced by $Mg(NO_3)_2 \cdot 6H_2O$ during lignin carbonization as templates to obtain carbon nanofibers with high SSA (628.09 $m^2\ g^{-1}$), high mesoporosity, and flexibility, and reached a specific capacity of 1135.4 mAh g^{-1} at a high current density of 2 C. After 100 cycles in a Li-ion battery, it still maintained the specific capacity of high specific capacity of 1064.7 mAh g^{-1} with 93.8% capacity retention. Wang et al.[65] prepared high microporosity lignin-based carbon materials with a maximum specific surface area of 1194.6 $m^2\ g^{-1}$ by using the KCl hard template.

For salt templates, the interaction between them and lignin is weak, so in order to increase the carbon material's porosity, an activator is always required. Therefore, the hard template can also be used in combination with chemical activation to increase the SSA of the carbon and to introduce a large number of micropores into the carbon. Xie et al.[66] employed a dual approach, utilizing both the NaCl template method and KOH activation, to synthesize porous carbon with a SSA of 3505 $m^2\ g^{-1}$ and a total pore volume of 2.0 $cm^3\ g^{-1}$ with a well-developed mesoporous microporous system.

In recent years, it has become an increasing trend to use multiple hard templates to prepare carbon material. Wu et al.[67] prepared carbon materials with 555 $m^2\ g^{-1}$ specific surface area using calcium

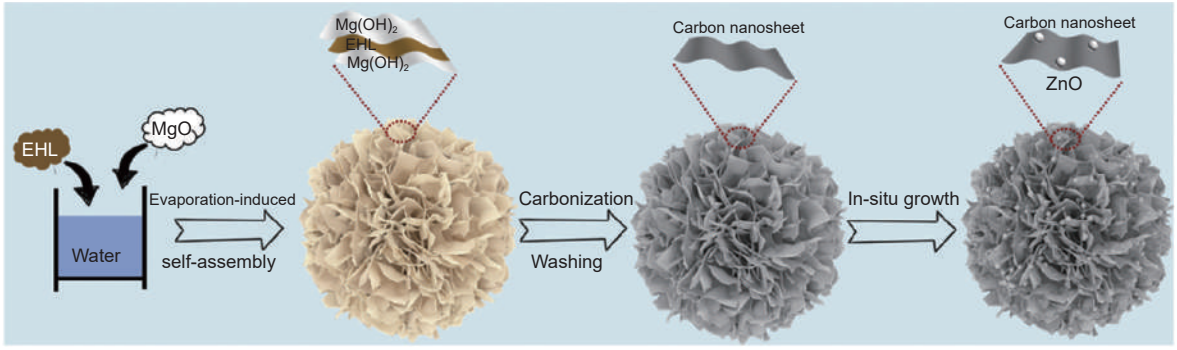

Fig. 5 Schematic diagram of preparation of ZnO@lignin-derived flower-like carbon composites using MgO as template. Adapted with permission from ref.[63]. Copyright 2020, Elsevier

lignosulfonate as raw material and $CaCl_2$ and SiO_2 as dual templates. Compared with $CaCl_2$ (712 m^2 g^{-1}) and SiO_2 (476 m^2 g^{-1}) single-template method, the dual templates of SiO_2 + $CaCl_2$ significantly increased the SSA and pore volume of mesopores and macropores. The authors also investigated the promotion effect of SiO_2 spheres on the growth of $CaCl_2$ crystal and their influence on the pore structure of the product, establishing a theoretical foundation for the standardized manufacturing of porous carbon on an industrial scale.

In summary, for the template method, the pore-forming effect of a single soft or hard template agent is often unsatisfactory, necessitating the use of dual templates or the addition of activators. However, this method has low requirements for production equipment and low costs for template agents, making it of great significance for the industrial production of lignin-based porous carbon.

2.3 Hydrothermal

The hydrothermal method involves heating a precursor in a sealed pressure vessel with water as a solvent to produce hydrocarbons at a relatively low temperature (130–250 °C) and pressure (self-produced pressure of 1–5 MPa). The physical properties of water undergo significant changes under hydrothermal conditions compared to those at room temperature and pressure, particularly with respect to thermal conductivity. Additionally, water and non-polar hydrocarbon mixed poorly at room temperature and pressure, but in hydrothermal conditions, water and nonpolar gaseous and liquid hydrocarbons were miscible. This unique property allows water to have multiple identities as a solvent, reactant, and catalyst in hydrothermal processes. Due to its ability to stabilize the initial microstructure and provide a mild environment for modulating microstructure, hydrothermal method has been widely used to synthesize advanced materials, such as carbon-based catalysts, which possesses improved stability and activity[68–71].

For lignin, in hydrothermal process, several chemical reactions such as hydrolysis, dehydration, decarboxylation, condensation, polymerization, and aromatization, occur. Under the conditions of hydrothermal, C—O bonds in lignin fractured and then formed a more stable, rigid and cross-linked carbon structure. Meanwhile the aromatic structure in lignin is much more stable. Therefore, the yield of carbon from lignin hydrothermal method is higher compared to cellulose and hemicellulose[72].

However, due to the low temperature of hydrothermal technique, the prepared carbon material was not completely carbonized, and the resulting porous carbon had a low specific surface area, undeveloped pores and poor electrical conductivity[73]. Therefore, hydrothermal carbonization holds greater promise as a pretreatment method. This means that further activation can enhance the electrochemical properties of porous carbon prepared by the hydrothermal method[74]. Li et al.[75] used a combination of hydrothermal (220 °C) and chemical activation (KOH, 80 g L^{-1}, 800 °C) to prepare a 3D structure porous carbon with a reasonable pore size distribution. The corresponding supercapacitor had a large specific capa-

citance of 324 F g^{-1} at a current density of 0.5 A g^{-1}, with 99.7% capacitance retention after 5000 cycles. Jain et al.[76] reported the application of hydrothermally assisted activation in converting black liquor, a by-product of the kraft pulping process, directly into activated carbon. This eliminated the steps for extracting and pre-carbonizing lignin. This provides a sustainable solution for large-scale production of carbon-based materials, specifically lignin-based carbon. A comparative analysis between black liquor activated carbon (BLAC), acid-washed black liquor lignin derived activated carbon (ABLAC), and commercial lignin-derived activated carbon (SALAC) showed that BLAC exhibited well-developed microporous and mesoporous structures and a significantly higher SSA of 2277.2 m^2 g^{-1}. BLAC also showed excellent specific capacitance of 871.4 F/g at a current density of 1 A/g, with low resistance values including an R_s of 1.37 Ω and R_{CT} of 0.05 Ω, demonstrating its high stability and efficiency when used as an active material for supercapacitors. According to Wang et al.[77], lignin nanospheres were initially fabricated through a two-step procedure involving self-assembly followed by hydrothermal treatment. Subsequently, they were chemically activated to prepare monodisperse, blueberry-like porous lignin-based carbon nanospheres (Fig. 6). They has a high SSA range of 557.9–2237.9 m^2 g^{-1} and when tested in a 3-electrode system, they exhibited excellent electrochemical behavior with a capacitance of 254.2 F g^{-1} at a current density of 0.2 A g^{-1}, an energy density of 6.3 Wh kg^{-1}, a power density of 3.4 kW kg^{-1}, as well as a long cycling stability after 10 000 cycles.

Except for post-activation treatment, adding catalysts during the hydrothermal process is also one of the directions that researchers have explored to improve the hydrothermal method. Most of these catalysts are aimed at increasing carbon yield rather than porosity. Although this is beneficial for industrial production, the disadvantage of underdeveloped pores in hydrothermal carbons remains unsolved. However, such work has mainly focused on the hydrothermal treatment of cellulose, with relatively less attention given to lignin[78–79]. Therefore, there are few types of catalysts for the hydrothermal treatment of lignin, with almost only one type available – $ZnCl_2$. Wu et al.[80] successfully synthesized hierarchical porous carbon by hydrothermal pretreatment of lignin with $ZnCl_2$, followed by KOH activation. The results showed that $ZnCl_2$ created some pores in the hydrothermal carbon, which promote the entry of KOH. The SSA of the hierarchical porous carbon was in the range of 1097–2955 m^2 g^{-1}. Among them, the porous carbon obtained by adding 50 mL of 5 mol L^{-1} $ZnCl_2$ solution to the hydrothermal treatment and activated at 600 °C showed the most excellent electrochemical properties, with a specific capacitance of 384 F g^{-1} at a current density of 40 mA g^{-1}, which was also maintained at 239 F g^{-1} at 5 A g^{-1}.

In summary, although the hydrothermal method cannot directly yield porous carbon with developed pores, it still has the following advantages as a promising pretreatment method: (1) Low temperature and low energy consumption are required for hydrothermal treatment. (2) Hydrothermal method has lower requirements for equipment, and the reaction processes involved are green and environmentally friendly. (3) The carbon obtained by hydrothermal treatment could maintain the microscopic morphology of the precursor. (4) There are abundant oxygen-containing functional groups on the surface of the carbon materials obtained by hydrothermal, which can be used as electrode materials of supercapacitors to increase the pseudocapacitance.

3 Activated carbon for supercapacitor application

3.1 Pores and pore structure

For supercapacitors, capacitance is the most important parameter. Generally it is assumed that the capacitance follows that of a parallel plate capacitor (EDLC) and the capacitance can be calculated by the equation (I).

$$C = \frac{\varepsilon_0 \varepsilon_r A}{d} \quad \text{(I)}$$

where ε_0 is the permittivity of a vacuum, ε_r is the

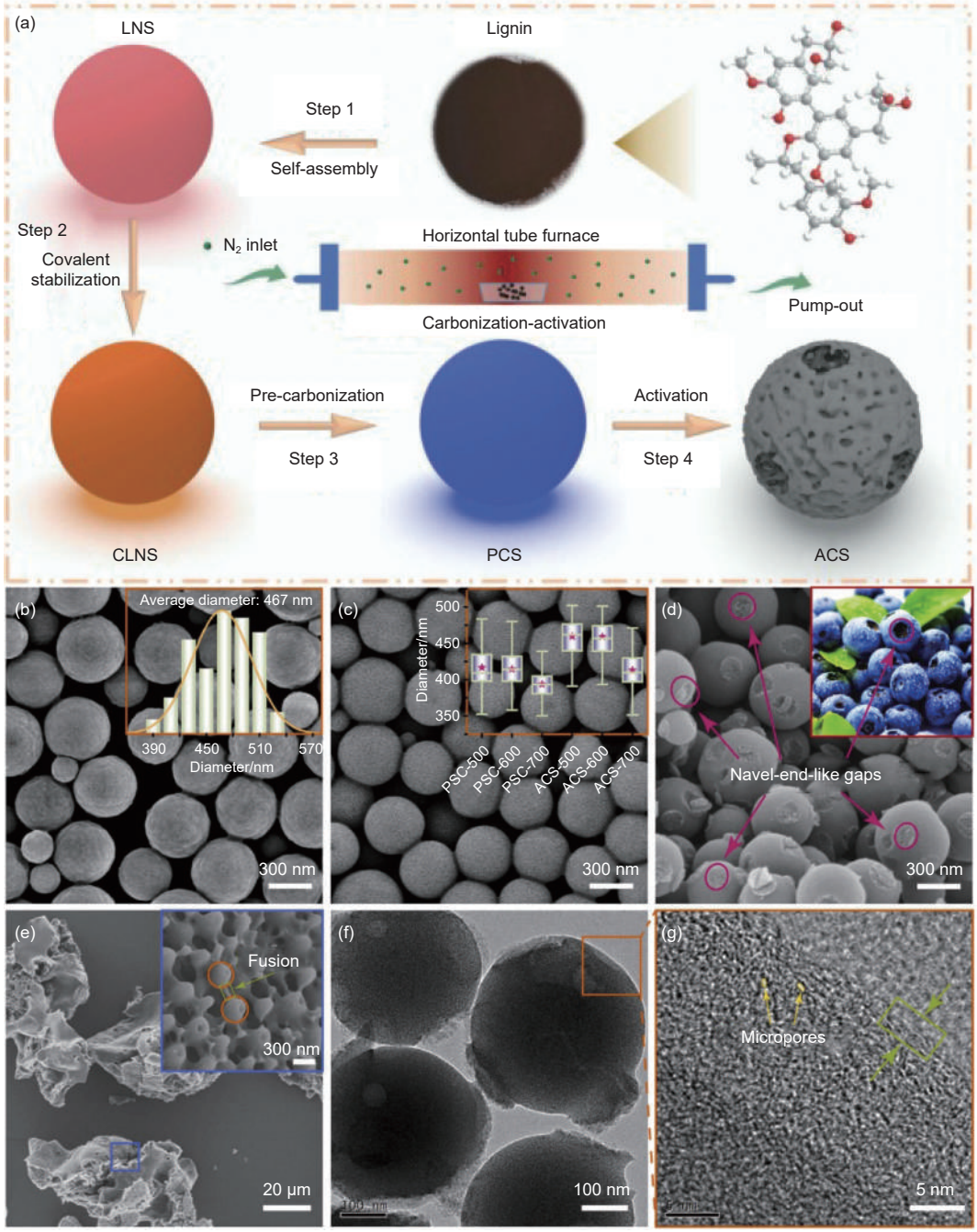

Fig. 6 (a) Schematic illustration of the preparation of ACS. (b)SEM image of lignin nanospheres (CLNS). (c) SEM image of lignin-based carbon nanospheres at the carbonization temperature of 600 °C (PCS-600). (d) Lignin-based porous nanospheres derived from PCS-600. Inset of (b, c and d) are the diameter distribution of CLNS, the diameter of various PCS and ACS, and the picture of blueberry, respectively. (e) SEM image of activated lignin-based carbon materials obtained from the pre-carbonization temperature at 400 °C. The inset in (e) is the magnified view of the blue rectangle. (f) HR-TEM image of ACS-600 and (g) a magnified view of ACS-600. Adapted with permission from ref.[77]. Copyright 2022, Elsevier

electrolyte dielectric constant, A is the actual area of the electrode forming the double layer, *d* is the interfacial distance between the electrolyte and the porous electrode. According to equation (I) porous carbon with more micropores usually has higher SSA and higher specific capacitance. Nevertheless, this model disregards the effects of pore curvature and inter-pore wall distances on the behavior of electrolyte ions, indicating that the real situation is significantly more complex than what the model implies. For macropores with diameters greater than 50 nm, the electrical double layer model can well explain the capacitance at the carbon/electrolyte interface, but it fails to reflect the pore curvature and inter-pore wall dis-

tances of mesopores and micropores. The most classic cases are the abnormal increase in capacitance when the pore diameter is less than 1 nanometer and the slight increase in capacitance when the pore diameter is greater than 2 nanometers[81].

To solve this problem, Huang et al.[82–83] proposed the EDCC (electric double-cylinder capacitor, Fig. 7(a) and EWCC (electric wire-in-cylinder capacitor, Fig. 7(b) models to separately account for the contributions of mesopores and micropores to capacitance. For mesopores, they assumed that the mesopores are approximately cylindrical, solvated cations and anions enter the pores and come close to the pore walls to form EDCCs. The capacitance of the EDCC can be given by equation (II)[82–83].

$$C = \frac{\varepsilon_0 \varepsilon_r \mathrm{A}}{b \ln(b/b-d)} \tag{II}$$

where b is the radius of the outer cylinder, and d is the distance between the ions and the surface of the carbon electrode (effective size of the counterion). For micropores, the small pore size does not allow for the formation of a double cylinder. So they assumed a cylindrical micropore, where only few solvated (or desolvated) counterions enter the pore and arrange to form an EWCC. The capacitance of the EWCC can be obtained from equation (III)[82–83].

$$C = \frac{\varepsilon_0 \varepsilon_r \mathrm{A}}{b \ln(b/a_0)} \tag{III}$$

where a_0 is the radius of the inner cylinder, it also represents the radius of the solvated (or desolvated) counterions. Equation (II, III) are only applicable to unimodal pores. For pores with multimodal pore size distributions, the contributions of macropores, mesopores, and micropores to the capacitance should all be included. The capacitance can be represented by equation (IV)[82–83]:

$$C = \sum_i \frac{\varepsilon_0 \varepsilon_{r,micro} \mathrm{A}_{i,micro}}{b_i \ln(b_i/a_0)} + \sum_j \frac{\varepsilon_0 \varepsilon_{r,meso} \mathrm{A}_{j,meso}}{b_j \ln\left[b_j/(b_j-d)\right]} + \sum_k \frac{\varepsilon_0 \varepsilon_{r,macro} \mathrm{A}_{k,macro}}{d} \tag{IV}$$

Researchers are now able to select different models based on actual situations to achieve satisfactory matches between the calculated results of the EDCC and EWCC models and experimental results for almost all types of carbon materials and electrolytes. To sum up, based on this theory, all pore sizes—macropores, mesopores and micropores—contribute to the overall capacitance. However, the contribution from micropores is notably significant due to the desolvation of certain electrolyte ions within these smaller pores.

Besides capacitance, energy density and power density are also important performance parameters in the development of high-performance capacitors. In the development of supercapacitor electrodes aimed at achieving higher energy density, it's crucial to focus on the formation of micropores, as energy density is directly proportional to capacitance. However, for electrodes with high power density requirements, the diffusion rate of the electrolyte on the electrode should be given more attention. It should be noted that micropores will significantly hinder the transfer of electrolyte, resulting in low utilization rate of specific

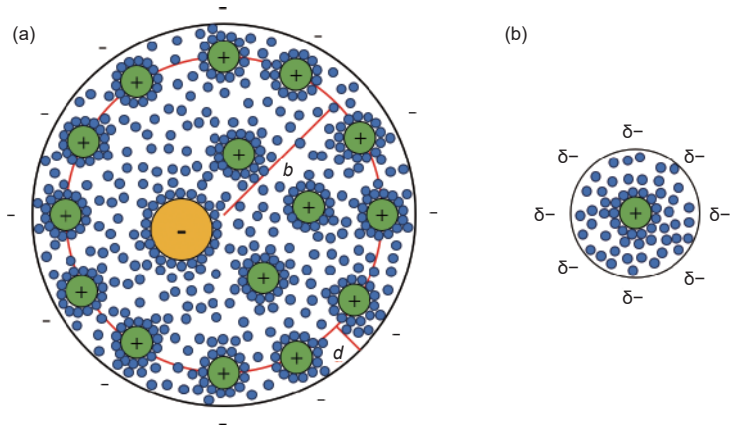

Fig. 7 Schematic diagrams of (a) EDCC and (b) EWCC

surface area and poor power density[50,84]. Consequently, the creation of porous carbon materials with a hierarchical pore structure is feasible, allowing for the combination of high energy density characteristic of micropores with the high power density associated with mesopores[85]. A pore structure with a reasonable proportion of micropores and mesopores can not only connect micropores to achieve the maximum specific active surface area, high specific capacitance, and high energy density, but also form a network of channels to connect micropores, thereby improving mass transfer rates and thus obtaining a high power density[86]. This is also the main direction of research efforts in recent years to optimize the porous carbon structure. According to Han et al.[87] that materials featuring a well-balanced distribution of pore diameters can facilitate the creation of additional ion pathways for both ion diffusion and storage, and hierarchical pores can effectively enhance the electrochemical properties of porous carbon in supercapacitors. Zhao et al.[88] used lignosulfonate as precursor and taking advantage of its abundant functional groups (—OH, $-SO_3Na$, —COOH, etc.), introducing potassium carboxylate into lignin, and using KCl, carbonate, and sulfate generated during carbonation as multiscale templating agents during pore formation. These multiple templates enable lignin to synthesize hierarchical porous carbon with high SSA (1784–2460 $m^2\ g^{-1}$). It also showed superior electrochemical properties when used as an electrode in supercapacitors. The Zn//LHPCs hybrid supercapacitors achieved an ultrahigh energy density of 135 Wh kg^{-1} at a power density of 101 W kg^{-1} (Fig. 8).

With the development of in-situ characterization techniques in recent years, researchers have been able to use experiments to explore in more detail the energy storage process and mechanism of porous carbon electrodes in supercapacitors. In fact, Levi et al.[89] pioneered work in this area as early as 2009. They used a quartz-crystal microbalance (QCM) as a weight probe to measure the ion adsorption and desorption processes in the pores of porous carbon electrodes. Since the adsorption and desorption of ions in the pores of porous electrodes do not alter their rigid nature but only change the vibrational frequency of the quartz crystal, the frequency change caused by ion adsorption directly reflects the mass change of the electrode. By monitoring the frequency change in real-time, the adsorption and desorption processes of ions on the electrode surface can be studied, thereby opening up a novel research method for investigating the energy storage mechanism of supercapacitors. However, the mass changes measured by QCM are difficult to accurately attribute to the mass changes of cations, anions, or solvent molecules, which poses an obstacle to further understanding the energy storage mechanism of supercapacitors. In-situ nuclear magnetic resonance (in-situ NMR) is a recently developed effective method for studying the energy storage mechanism of supercapacitors. Grey et al.[90] established an in-situ NMR method for investigating the energy storage mechanism of supercapacitors, which can track the ion concentration in the pores of porous electrodes at different operating voltages in real-time. In NMR experiments, ions and solvent molecules in the pores and in the bulk phase exhibit different NMR peaks. By tracing different NMR nuclei, cations, anions, and solvent molecules can be studied separately. As long as ions are adsorbed inside the carbon pores, they will cause similar chemical shift changes. Therefore, NMR can measure the number of ions in the carbon pores by fitting the spectra, making it an effective method for quantitative study of ion adsorption and desorption in the pores.

In addition to using in-situ QCM and NMR, in-situ X-ray photoelectron spectroscopy(in-situ XPS)is also an effective tool for exploring the energy storage mechanism of supercapacitors. Kruusma et al.[91–92] investigated the electrochemical processes of Mo_2C-derived carbon ($C(Mo_2C)$) electrodes in an electric double-layer capacitor (EDLC) using 1-ethyl-3-methylimidazolium tetrafluoroborate ($EMImBF_4$) ionic liquid at different cell potentials through in-situ XPS. Consequently, the relationship between the supercapacitor cell potential and the in-situ XPS signals was analyzed, and potential electrochemical reactions

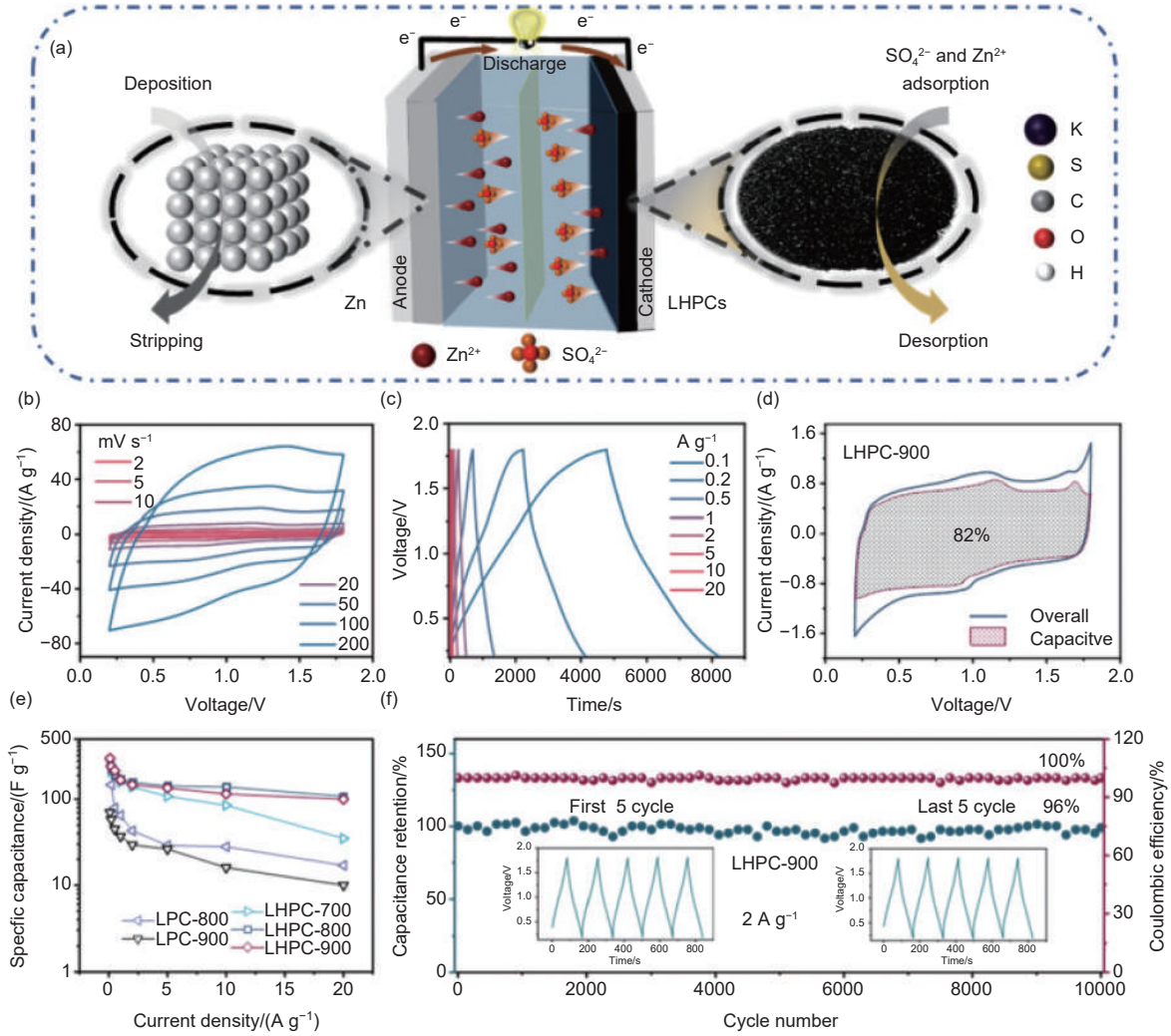

Fig. 8 (a) Schematic illustrating the configuration of ZHISCs. (b) CV curves of LHPC-900 at different scan rates. (c) Charge/discharge curves at different current densities of LHPC-900. (d) Contribution of capacitance and diffusion-controlled charge storage processes. (e) Charge/discharge rate performance of LPC-800, LPC-900 LHPC-700, LHPC-800 and LHPC-900. (f) Long-term cycle performance of LHPC-900 at a current density of 2 A g^{-1}.
Adapted with permission from ref. [88]. Copyright 2022, Elsevier

occurring at the interface between the working electrode and the ionic liquid under the applied extreme EDLC cell potentials were identified.

In-situ characterization methods are not only useful for exploring energy storage mechanisms; Chen et al.[93] utilized in-situ TEM to examine the dynamic behavior of porous carbon electrodes during the electrochemical cycling of supercapacitors in real time. Elevating the potential beyond a specific threshold during cycling caused gas evolution, which initiated a series of reactions that ultimately led to the decomposition of the porous carbon. This manifested as mass loss in the electrode and a rapid decline in capacity upon further cycling. They discovered that applying a nanolayer oxide coating to the porous carbon electrode by atomic layer deposition effectively inhibited electrode-electrolyte interactions, stabilized the electrode, and enhanced its electrochemical properties. Their research marked a significant advancement in comprehending the degradation of supercapacitors and offered a practical approach for examining electrode dynamics across a range of energy storage systems.

Several specific approaches have been suggested for modulating the pore structure, including adjusting the amount or type of activator, activation temperature, type or concentration of templating agent, etc. Taslim et al.[94] obtained porous carbon through physical activation using CO_2. The activated carbon, after

optimization, has a high porosity and a rich three-dimensional hierarchical pore structure, with microporous and mesoporous areas of 76.98% and 23.02%, respectively. In addition, the electrochemical performance in a symmetric supercapacitor displayed a high specific capacitance of 202 F g^{-1} at a current density of 1 A g^{-1}, with an excellent energy density of 11.61 Wh kg^{-1} at a power density of 156.71 W kg^{-1}. Zhang et al.[95] synthesized active carbon sheets using KOH and adjusted the ratio of microporous to mesoporous by changing the ratio of KOH/C. This process yielded activated carbon sheets with remarkable specific capacitance and energy density (447 F g^{-1} at 0.5 A g^{-1} and 15.5 Wh kg^{-1} at 62 W kg^{-1}), along with excellent cycling stability, retaining 95% of their capacitance after 10 000 cycles. Boric acid can also serves as an innovative activator that can effectively regulate the pore structure of porous carbon. Li et al.[96] designed an eco-friendly method utilizing boric acid to prepare hierarchical porous carbon derived from agaric. The porous carbon possesses an excellent SSA of 2279.5 m^2 g^{-1}, a more rational hierarchical pore structure, and a large specific capacitance of 502 F g^{-1} at a current density of 0.5 A g^{-1}. Zhu et al.[97] designed a method for synthesizing lignin-based hierarchical mesoporous carbon with a high SSA, employing a sustainable nano-$CaCO_3$ as a hard template. It provides a new idea for the industrial production of lignin-based porous carbon. In this process, the recovery rate of nano-$CaCO_3$ can reach 90%. In addition, the CO_2 produced by the pyrolysis of the nano-$CaCO_3$ template is used as an activation gas in the carbonization process, which has an internal activation effect on the carbon material, resulting in the generation of micropores and the expansion of pore size. The SSA of lignin-based porous carbon prepared by this strategy was as high as 860.5 m^2 g^{-1}, and the mesoporous volume accounted for more than 90% of the total pore volume. When used as the cathode of a zinc-ion hybrid supercapacitor, the capacitance retention rate is as high as 64% when the current density increased from 0.1 to 20 A g^{-1}.

Another way to regulate the structure of lignin-based porous carbon is through changing the morphology of precursors to obtain carbon with specific morphologies. The most common of these is carbon nanofibers[99–102]. Carbon fiber has the advantages of high strength, high modulus, light weight, heat resistance, so it has been widely used in flexible capacitors in recent years[103–104]. Ma et al.[98] prepared microporous carbon nanofiber membranes (MCNMs) by electrospinning using TEOS as a template agent (Fig. 9). At a TEOS/lignin mass ratio of 2∶1, the resulting carbon nanofibers exhibited the maximum specific surface area (1197 m^2 g^{-1}) and high microporosity (84.1%). Lignin-based MCNMs have good flexibility and strength, and exhibit a significant specific capacitance (282 F g^{-1} at 0.2 A g^{-1}) when used as self-supporting electrodes in a three- electrode system. By assembling lignin-derive MCNMs layer by layer, a thick electrode (25.4 mg cm^{-2}) was constructed with a capacitance of 5.72 F cm^{-2}. Wang et al.[105] synthesized size-controlled carbon nanospheres derived entirely from lignin by self-assembly, stabilization treatment, and carbonization. The dimensions of the resulting carbon nanospheres can be modulated to fall within the range of 256 to 416 nm by altering the concentration of lignin. When assembled into a supercapacitor, it demonstrates a high maximum specific capacitance of 147 F g^{-1} at 0.5 A g^{-1}. Moreover, after undergoing 10 000 charge-discharge cycles, the capacitance retention remains at 85.37%, indicating excellent long-cyclic stability. According to Wang et al.[106], lignin and epichlorohydrin were combined by chemical crosslinking, and then activated with KOH to obtain lignin-based carbon aerogels (Fig. 10). It possesses an exceptionally high SSA of 3675 m^2 g^{-1}, which contributes to its remarkable specific capacitance of 504.7 F g^{-1} in a three-electrode system at 0.2 A/g. According to Feng et al.[107], a range of lignin-derived porous carbons, each exhibiting unique particle shapes and hierarchical pore structures, have been synthesized through the processes of spray drying and subsequent KOH activation. In this work, lignin with different morphologies (sphere, dimple and shell) can be regulated by the temperature of spray drying. The result shows that

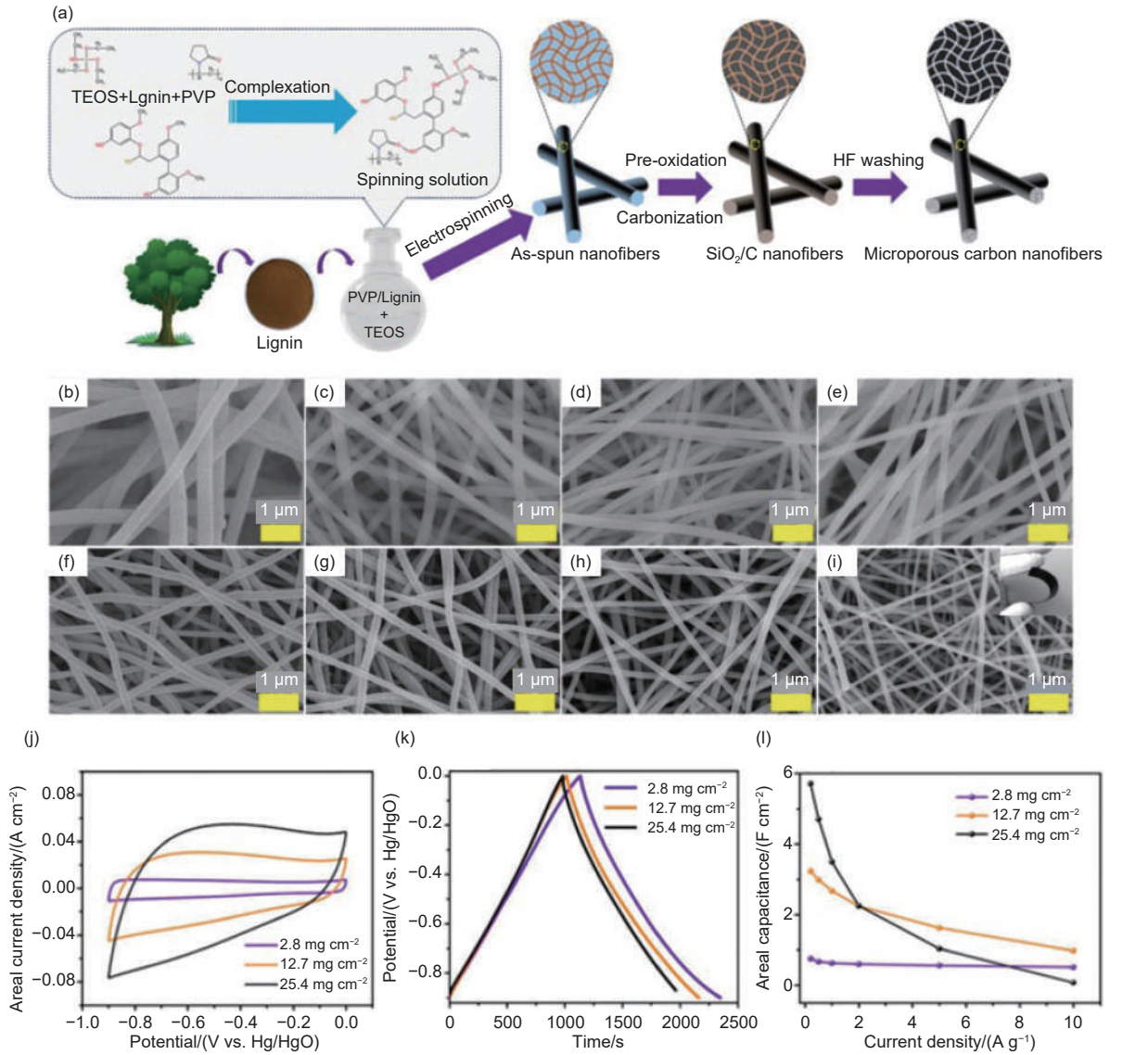

Fig. 9 (a) Schematic of the fabrication procedure of LCNF-T-Xs. (b-i) SEM images of LCNF-T-Xs. (j) CV curves at 10 mV s^{-1}. (k) Charge/discharge curves at 0.2 A g^{-1}. (l) Areal capacitance with various current densities. Adapted with permission from ref.[98]. Copyright 2024, Elsevier

spherical had higher SSA, higher specific capacitance and excellent rate capability (372.5 F g^{-1} at 0.2 A g^{-1} and 264.8 F g^{-1} at 20 A g^{-1}).

3.2 Heteroatom dopant

The electrochemical performance of carbon materials is also affected by their surface properties, such as heteroatoms (nitrogen, oxygen, sulfur, phosphorus, and boron, etc.) can improve the hydrophily of carbon in aqueous electrolytes, in addition, some functional groups containing oxygen and nitrogen can provide additional capacitance to improve the electrode materials' electrochemical performance. The doped atoms have a radius close to that of carbon atoms and possess different electronic structures (Fig. 11)[108]. According to the theoretical calculations by Gao et al.[109], doping with p-block elements (B, N, O, P and S) can facilitate proton adsorption by reducing the minimum Gibbs free energy of adsorption $\Delta G_{H^*}^{min}$ on carbon. In their theory, the capacitance of the unit charge storage site, denoted as $C_{0/site}$, can be approximately expressed by equation (V)[109].

$$C_{0/site} = \frac{\frac{1}{2}e^2\left(\frac{eU-\Delta G_{H^*}^{min}}{\Delta G_{H^*}^{max}-\Delta G_{H^*}^{min}}\right)^2}{\frac{eUk_BT}{eU-\Delta G_{H^*}^{min}}ln\left[\frac{1}{2}\left(1+e^{\frac{eU-\Delta G_{H^*}^{min}}{k_BT}}\right)\right]} \quad (V)$$

where U is the external electric potential, e is the charge of electron, k_B is the Boltzmann constant, and T is the temperature. According to equation (VI) and

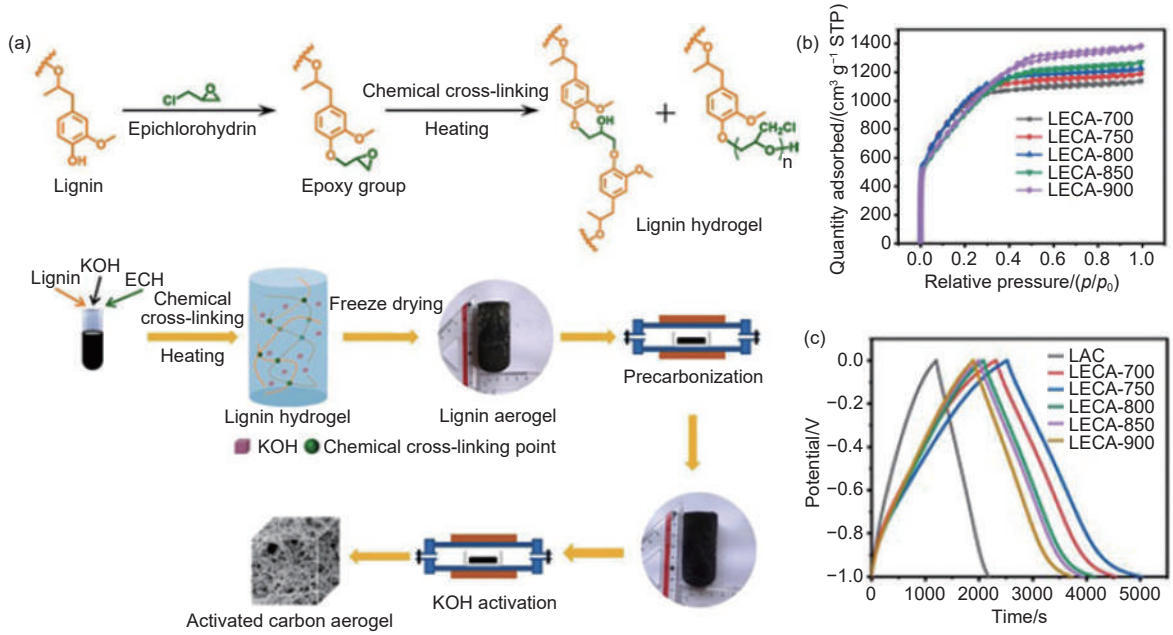

Fig. 10 (a) Schematic illustration of the LECA synthesis process. (b) Nitrogen adsorption–desorption isotherms. (c) GCD curves at 0.2 A g^{-1} of the LECAs using 6 mol L^{-1} KOH as the electrolyte. Adapted with permission from ref. [106]. Copyright 2023, Elsevier

(VII), the reduction in the $\Delta G_{H^*}^{min}$ implies that doping will simultaneously improve both the energy density ($E_{0/site}$) and power density ($P_{0/site}$) of supercapacitors[109].

$$E_{0/site} = \frac{eUk_BT}{eU-\Delta G_{H^*}^{min}} ln\left[\frac{1}{2}\left(1+e^{\frac{eU-\Delta G_{H^*}^{min}}{k_BT}}\right)\right] \quad (VI)$$

$$P_{0/site} = k_0 \times \frac{eUk_BT ln\left[\frac{1}{2}\left(1+e^{\frac{eU-\Delta G_{H^*}^{min}}{k_BT}}\right)\right] - \frac{1}{2}(\Delta G_{H^*}^{min}-eU)^2}{\Delta G_{H^*}^{max}-\Delta G_{H^*}^{min}+k_BT\left(e^{\frac{\Delta G_{H^*}^{max}-eU}{k_BT}}+e^{\frac{\Delta G_{H^*}^{min}-eU}{k_BT}}\right)} \quad (VII)$$

Furthermore, they also predicted that N and S elements will be the best doping elements, which is highly consistent with current research results on carbon doping.

Due to the inherent presence of oxygen in lignin, the research on oxygen dopants in lignin-based carbon is the most common. In addition, the existence of multiple functional groups (—OH, —O— and —OCH_3) and the manufacturing technique of lignin (Kraft process) make doping of N and S elements more convenient[110]. However, too high a content of heteroatoms also affects the electrical conductivity of carbon and the cycle life of supercapacitors. Therefore, it is important to dope the carbon with an appropriate amount of heteroatoms to obtain higher electrochemical performance. The content of heteroatoms typically depends on the carbonization method and doping process. The doping process can be broadly categorized into three types: doping before carbonization, doping during carbonization, and doping after carbonization. As shown in Table 4, the best doping effect is achieved when the dopant is added during the carbonization process, and some dopants inherently possess certain activating properties, eliminating the need for additional activators during carbonization. The doping effect is generally moderate when heteroatoms are introduced into the precursor before carbonization, primarily because the chemical bonds between the heteroatom groups and the precursor are not strong enough, and significant loss of doping atoms occurs during the intense activation. The worst doping effect is observed in post-doping, mainly because the carbon structure, having undergone high temperatures, becomes very stable, making it difficult for dopants to penetrate into the carbon lattice. For biomass-derived carbon doping, current research primarily focuses on the first two processes. Thus, future research should aim to develop dopants with activating capabilities to simplify the process flow.

3.2.1 N doping

For nitrogen, through DFT simulations, research-

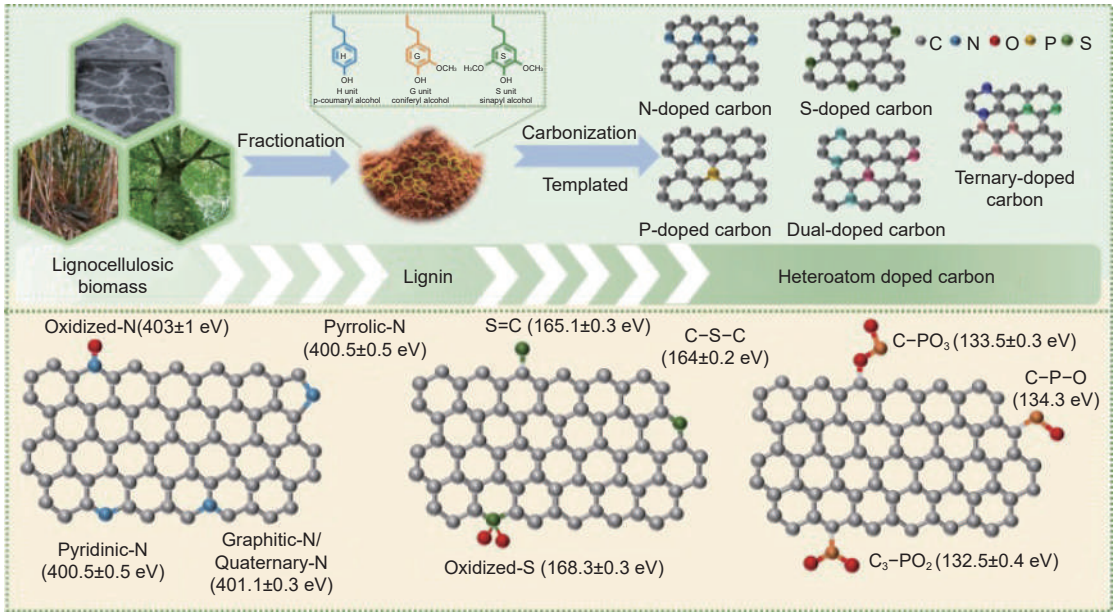

Fig. 11 Schematic diagram of the structure of lignin-based carbon doped with different heteroatoms. Adapted with permission from ref. [108]. Copyright 2024, Elsevier

Table 4 The parameters comparison of lignin-based porous carbon prepared by different doping methods

Types of carbon	Carbonization strategy	Dopant	Doping element	Element content/ %	Electrochemical test conditions	Specific capacitance/ (F g^{-1})	Capacitance retention	Ref.
Nanospheres	Doping during carbonization No other agents	Urea	N	8.4	6 M KOH 3-electrode system	232 at 0.5 A g^{-1}	97.2% after 10000 cycles at 20 A g^{-1}	[114]
Nanosheets	Doping during carbonization No other agents	$Cu(NO_3)_2·3H_2O$	N O	6.7 11.2	1 M $ZnSO_4$ ZIHC(Zn//C)	301 at 0.1 A g^{-1}	-	[115]
Hierarchical porous carbon	Doping before carbonization Fe_3O_4 (template) and KOH (activator)	Ethanediamine	N S	1.4 1.8	6 M KOH 3-electrode system	241 at 1 A g^{-1}	95.0% after 3000 cycles at 10 A g^{-1}	[120]
Hierarchical porous carbon	Doping before carbonization MgO (template) and KOH (activator)	KSCN	N S	1.3 0.4	1 M $ZnSO_4$ ZIHC(Zn//C)	295 at 0.2 A g^{-1}	99.0% after 10000 cycles at 5 A g^{-1}	[121]
Hierarchical porous carbon	Doping before carbonization KOH (activator)	Urea	O N S	15.4 2.6 1.2	6 M KOH asymmetric supercapacitor	110 at 0.5 A g^{-1}	99.6% after 10000 cycles at 1 A g^{-1}	[122]
Porous carbon	Doping after carbonization KOH (activator)	Boric acid	B	4.0	3 M KOH 3-electrode system	285.6 at 1 A g^{-1}	98.0% after 5000 cycles at 5 A g^{-1}	[124]
Porous carbon	Doping before carbonization No other agents	$NH_4B_5O_8·4H_2O$	B N	13.1 16.7	6 M KOH symmetric supercapacitor	91 at 0.5 A g^{-1}	91.0% after 10000 cycles at 1 A g^{-1}	[126]

Note: M: mol L^{-1}

ers have shown that N doping significantly enhances the polarity of carbon surfaces. This increase suggests that N doping induces substantial polarization on the carbon surfaces, which in turn boosts the interaction between the electrode and the electrolyte, as well as enhances the wettability of the electrodes[111–112]. Additionally, N has an atomic radius closely resembling with C, which helps to minimize the exist of lattice mismatches. N doping has the additional advantage of stopping the formation of hydrocarbons in the lattice and preventing the generation of hydrocarbon dielectric dead layer, which can reduce the performance of supercapacitors[113]. According to DFT calculations, among the three bond types of nitrogen (N-Q, N-5 and N-6), N-5 exhibits the best adsorption performance of electrolyte ions. Therefore, the future direction for improving nitrogen doping should focus on increasing the proportion of N-5. According to Yang et al.[114], N-doped lignin-based carbon nanospheres were successfully synthesized using lignin nanospheres as the carbon source and urea as the nitrogen source. The N content and carbonization temperature of urea significantly improve the physicochemical properties of the carbon. Testing in a 3-electrode system, 8.4% N con-

tent of the carbon materials exhibited the highest capacitance of 232 F g^{-1} (at 0.5 A g^{-1}) and long cycling stability (retention of 97.2% after 10 000 cycles). Compared to the undoped lignin-based carbon nanospheres, it increased about 40% in specific capacitance. Wen et al.[115] prepared lignin-based N/O codoped 3D hierarchical porous carbon nanosheets by one-step using $Cu(NO_3)_2$ as dopant and templating agent. It shows that N doping can improve the pseudocapacitive response by reducing the energy barrier for oxidation state changes in the carbonyl part. The constructed zinc-ion supercapacitors exhibit both high specific capacitance (301 F g^{-1} at 0.1 A g^{-1}) and remarkable rate capability (maintaining 30% capacitance at 200 A g^{-1}). This can be attributed to the enhanced pseudocapacitance resulting from nitrogen and oxygen doping, as well as the rapid diffusion of Zn^{2+} ions within the 3D interconnected hierarchical porous carbon matrix. This synergistic effect of nitrogen and oxygen dopants in the 3D hierarchical porous carbon cathodes plays a crucial role in the ultra-fast zinc ion hybrid supercapacitors, leading to their superior electrochemical performance.

3.2.2 S doping

Sulfur is also considered a promising doping element in carbon materials. The overlap between the p orbital of S and the sp^2 orbital of C forms an extended p system with filled valence bands, which can increase the electrical conductivity of carbon. The dipole moment between S and C will increase with the action of the electric field, and the degree of polarization of the carbon is enhanced ultimately leading to an increase in the capacitance of the carbon material[116]. In addition, S atom inhibits pore shrinkage and the development of undesirable pores[117]. According to Gao et al.[109], N is the best dopant among p-block elements and S is the second-best dopant element, so N,S co-doped carbon should have good capacitive performance. In fact, it is exactly as expected, co-doped carbon even exhibits higher capacitance than any singly doped element. To further investigate the differences in co-doped structures, they chose 2 other dopant elements that are suboptimal in performance relative to N, forming an O, S co-doped graphene structure. The results indicated that the improvement of the capacitance performance of O and S co-doped carbon is not so large as N,S co-doped carbon. This is due to the fact that N/S co-doping in carbon materials produces a synergistic effect due to the high activity of different doping elements[118], which produces more active sites and favors the increase in pseudocapacitance. Chen et al.[119] further explored this synergistic effect through DFT calculations. N-5 has a tendency to push S atoms out of the plane of graphene, causing these S atoms to form sp^3 hybridization. Conversely, when pyridinic nitrogen (N-6) is present, S atoms stay within the graphene plane and form sp^2 hybridization. Furthermore, when S atoms are embedded in pyridinic-N-doped graphene, a new band close to the Fermi level is incorporated into the band structure, resulting in an increase of up to nearly 50% in the quantum capacitance of the co-doped graphene at low concentrations. However, when the doping concentration becomes too high and another N or S atom is embedded into the microstructure of the co-doped graphene, there is no significant enhancement in the quantum capacitance.

Yin et al.[120] prepared N/S co-doped carbon using sodium lignosulfonate and ethylenediamine, which conferred 3D pores of different scales using Fe_3O_4 as templating agent and KOH activation. The samples have a large SSA (1199 cm^2 g^{-1}) and specific capacity (241 F g^{-1} at 1 A g^{-1}), as well as a high energy density of 27.2 Wh kg^{-1} (at 10 000 W kg^{-1}), resulting in an excellent rate capability. Furthermore, the specific capacity remained at 95.0% after 3000 cycles, demonstrating excellent electrochemical stability. Fan et al.[121] used KSCN as dopant to prepare N and S co-doped lignin hierarchical porous carbon (NSLHPC). It shows a impressive specific capacitance of 438 F g^{-1} (at 0.5 A g^{-1}) and an excellent rate capability (226 F g^{-1} at 20 A g^{-1}) in a 3-electrode system. Moreover, the results of DFT calculations showed that co-doping with nitrogen and sulfur lowers the adsorption energy barrier for Zn^{2+} ions (Fig. 12). Thus, zinc-ion hybrid supercapacitor assembled by NSLHPC achieved a re-

markable energy density of 104.9 Wh kg^{-1} and a power density of 160.6 W kg^{-1} at a current density of 0.2 A g^{-1}. According to Shi et al.[122], O/N/S co-doped 3D hierarchical porous carbon was synthesized by using KOH and aminated enzymatic lignin. It was characterized by high SSA, developed pore structure, and high density of heteroatoms (O: 15.39%, N: 2.56% and S: 1.17%). As an electrode, it exhibits an elevated specific capacitance of 318 F g^{-1} (at 0.5 A g^{-1}) and an excellent rate capability of 62% (at 50 A g^{-1}) in a 3-electrode system. Asymmetric supercapacitors fabricated on this provided an energy density of 16.7 Wh kg^{-1}, a power density of 249 W kg^{-1}, and a capacitance retention of 99.58% after 10 000 cycles.

3.2.3 B doping

Boron, with its 3 valence electrons, is recognized as another p-type dopant, typically functioning as an electron acceptor when doped into a carbon matrix. This results in an elevated surface charge density and a subsequent increase in the specific capacitance of the carbon. As the increases of B content and the O-related functional groups, more active sites are generated on the surface of graphene, making it more hydrophilic in the electrolyte and thus exhibiting better electrochemical activity. Furthermore, the presence of an appropriate amount of B can promote redox reactions and increase the pseudocapacitance of B-doped graphene materials[123].

Poornima et al.[124] used wood as precursor and boric acid as the boron source to prepare B-doped porous carbon through a process of chemical activation followed by hydrothermal boron doping. The hydrothermal boron doping not only allows carbon to absorb some boron atoms but also increases the SSA of the carbon-based material. Due to the boron dopant, the prepared microporous carbon with 4% boron content has the largest SSA (1503.7 m^2 g^{-1}). This sample has the highest specific capacitance of 285.6 F g^{-1} at 1 A g^{-1} and an excellent cycling performance with 98% retention after 5000 charge-discharge cycles. The developed flexible asymmetric supercapacitor has an energy density of 87.7 Wh kg^{-1} and a power density of 4000 W kg^{-1}.

Due to the opposite electronegativity of B and N with respect to C, a new electronic structure can be introduced and structural distortions can be induced, resulting an enhancement in capacitance[125]. Luo et al.[126] prepared a series of nitrogen and boron co-doped wood-based porous carbon using a combination of microwave-assisted hydrothermal with pyrolysis. In pyrolysis process, they utilized $NH_4B_5O_8·4H_2O$ as the source for both boron and ni-

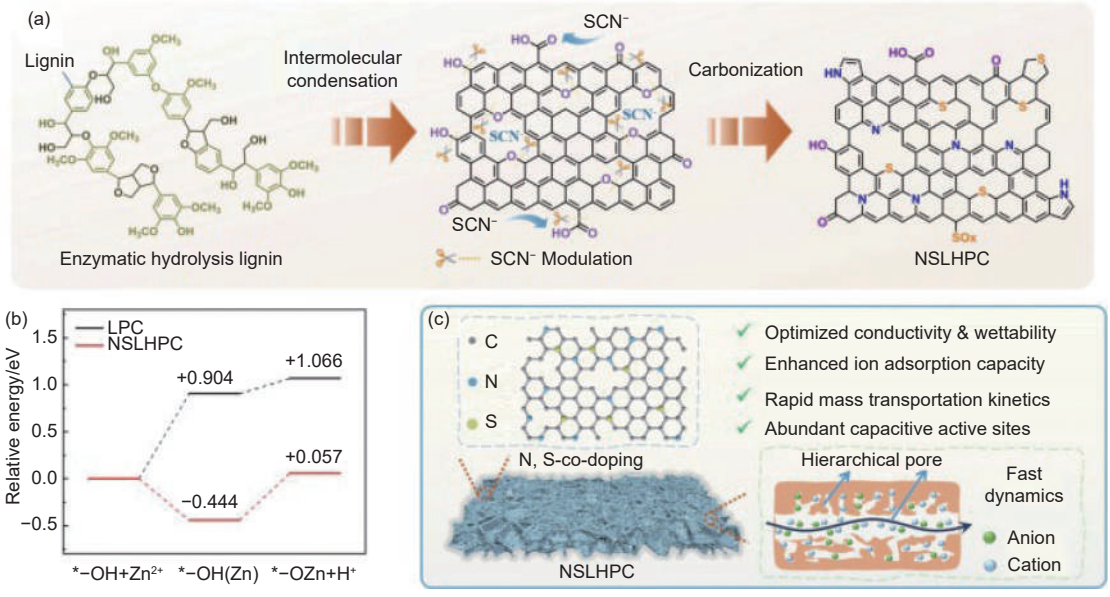

Fig. 12 (a) Schematic diagram of the mechanism of thiocyanate modulated lignin carbon surface. (b) Relative energy of chemisorption. (c) Mechanism schematic of NSLHPC as a working electrode. Adapted with permission from ref. [121]. Copyright 2024, Elsevier

trogen doping. These carbon materials are mainly microporous, with a SSA of 955 $m^2\ g^{-1}$, a B content of 10%–13%, and a N content of 15%–20%. The best electrode has a specific capacitance of 188 F g^{-1} at 0.5 A g^{-1}, which is twice that of the undoped carbon electrode, and maintains 90% capacitance retention after 10 000 cycles.

Moreover, the addition of borate and boric acid can significantly suppress the softening and swelling effects on lignin. This is crucial because many factors detrimental to carbonization are associated with the softening behavior of lignin during the pyrolysis process such as instability of preliminary pyrolysis products of lignin. This is because boric acid forms esters with phenolic hydroxyl groups[127], thereby reshaping the microstructure of the carbon precursor[128], and reducing the polymerization reactions that occur between lignin molecules during the hydrothermal process. Dong et al.[129] investigated the effects of boron compound (H_3BO_3, $Na_2B_4O_7$ and $K_2B_4O_7$) on lignin softening and compared them with $Ca(OH)_2$ and $Mg(OH)_2$. It was found that the boron additives were effective in inhibiting the aggregation of lignin molecules during the pyrolysis process. In their study, the boron compound promoted the carbonization of lignin, increased the yield of carbon, and inhibited the production of gaseous small molecules CO_2 and CH_4 and organic vapors, especially phenolic compounds.

3.3 Composite materials

3.3.1 Composite with transition metal compounds

Researchers have been deeply engaged in exploring the synthesis of carbon-based composites with transition metal compounds (metal oxides[130–131], metal sulfides[132], metal-organic framework[133]) to enhance the performance of electrode materials. Modification of lignin-based porous carbon with metal oxides not only generates more active sites, but also combines the excellent cycling stability of carbon materials with the high energy density of metal oxides, as well as combining pseudocapacitance and bilayer capacitance.

However, the mismatch between metal oxides and carbon materials can severely compromise their electrode performance. A major issue arises from inconsistent electrochemical reaction kinetics. During Faraday reactions, metal oxides often exhibit slow ion/electron transport, leading to capacity degradation at high rates. Moreover, the interface between metal oxides and carbon materials is crucial for charge transfer. Especially for composites prepared through ex-situ methods, the bond between carbon and metal oxides is not very tight. In this context, the design of novel interface structures becomes particularly important. Sui et al.[134] developed a carbon nanotube carpet (CC)/Fe_2O_3 nanoparticle composite covered with a bud-like carbon wrapper. The bud-like carbon wrapper expands the interface area and provides an accelerated conductive network through a "seamless" connection between CC and Fe_2O_3 nanoparticles, significantly enhancing charge transfer efficiency. Nevertheless, such interface designs are still relatively scarce for biomass-derived carbon, which should be a key focus for researchers in related fields in the future.

For composites prepared through in-situ methods, gaining an in-depth comprehension of the carbonization process is crucial for precisely controlling the microstructure of the interface in the final material. This understanding allows for the optimization of material properties and the enhancement of performance in various applications. Yue et al. analyzed the pyrolysis-induced structural alterations in MoO_x/carbon composites by employing a synergistic approach involving in-situ X-ray diffraction under heating conditions, along with simultaneous FTIR and TGA-MS (thermogravimetric analysis-mass spectrometry) experiments. They concluded that the improvement of cycle stability and coulombic efficiency of the molybdenum oxide/carbon nanocomposites can be ascribed to 2 factors. Firstly, the nanocomposite leads to a uniformly distributed conductive carbon phase, thereby boosting electronic conductivity. Secondly, the carbothermal reduction during the pyrolysis of the nanocomposites leads to the formation of MoO_2, which exhibits better cycle stability compared to MoO_3.

Shi et al.[135] successfully prepared hierarchical porous lignin-based carbon@WO_3. As a material for

supercapacitors, it can operate within a wide voltage range from 0.4 to 1.0 V. It shows a high specific capacitance of 432 F g^{-1} at 0.5 A g^{-1} and an excellent capacitance retention of 86.6% after 10 000 cycles at 10 A g^{-1}. The asymmetric supercapacitor constructed using this material delivers a remarkable energy density of 34.2 Wh kg^{-1} at a power density of 237 W kg^{-1} and 16 Wh kg^{-1} at a power density of 14 300 W kg^{-1}. Mu et al.[136] designed a composite material composed of layered porous carbon based on lignin-phenol-formaldehyde resin as a conductive skeletons and self-assembled $MnCo_2O_4$ as active sites. The composite material has a well-developed porous structure and excellent electrochemical properties, that means, more mass-transfer channels and redox-reacted active sites, and the maximum specific capacitance is up to 726 mF cm^{-2} at 0.5 mV s^{-1}. The all-solid-state asymmetric supercapacitor assembled with this material has the highest energy density of 0.68 mWh cm^{-3} and the power density of 8.2 mW cm^{-3}. In addition, the device exhibits a high capacitance retention of 87.6% after 5000 cycles at 5 mA cm^{-2}. Dai et al.[137] prepared Ni-Co-Ti compound co-dope lignin-derived carbon nanofiber (CNFs//TiO_2@$NiCo_2(OH)_6$). It shows an excellent specific capacitance of 752.47 F g^{-1} at 1 A g^{-1}. Furthermore, with an increase in current density to 10 A g^{-1}, the capacitance retention remained at 73.54%, indicating exceptional rate capacity retention. These results demonstrate the remarkable performance of the developed material in storage of electric charge. They also discovered that there is a synergistic interaction between TiO_2 and $NiCo_2(OH)_6$.

Metal sulfides have also attracted much attention in recent years as compelling pseudocapacitive material because of their higher electrochemical properties compared to metal oxides. The electronegativity of S is lower than that of O, and therefore electron leaps are more likely to occur in metal sulfides than in metal oxides[138–139]. Cao et al.[140] successfully loaded NiS nanoparticles onto sodium lignosulfonate-derived porous carbon using hydrothermal method, as shown in Fig. 13. The composite material tested in a 3-electrode system exhibited a high specific capacity of 677 C g^{-1} at 0.5 A g^{-1} and an excellent rate capability (297.8 C g^{-1} at 10 A g^{-1}). In addition, the asymmetric supercapacitor, assembled with this material, reached a peak energy density of 45.6 Wh kg^{-1} at a power density of 509.5 W kg^{-1}. It also displayed remarkable cycling stability, retaining 92.6% of its capacitance after 20 000 cycles at a current density of 2.5 A g^{-1}. Li et al.[141] successfully deposited $NiCo_2S_4$ nanoparticles in situ onto the inner surface of lignin-based porous carbon through a single-step solvothermal process, resulting in a high electrochemical performance in supercapacitors. The composite material produced a specific capacity of 1264.2 F g^{-1} at 1 A g^{-1} in a 3-electrode system. The asymmetric supercapacitor assembled by this material and active carbon provided an energy density of 32.05 Wh kg^{-1} at a power density of 193.9 W kg^{-1}.

3.3.2 Composite with conductive polymers

Conductive polymers are another common electrode material used in supercapacitors, and can be composited with carbon materials to prepare carbon@polymer electrodes[142]. Conductive polymers have the unique electrical properties like metals. The main reason behind this is the presence of conjugated π-electrons[143–144]. Among the most common conductive polymers are polypyrrole, polythiophene, polyaniline, and polyacetylene. The pseudocapacitance of conducting polymers stems mainly from the redox process as well as adsorption and desorption process, which occurs primarily during electron and ion transfer between the polymer and the electrolyte. Conductive polymers such as polypyrrole and polyaniline undergo reversible redox reactions during charging and discharging. These reactions involve the transfer of electrons, leading to changes in the charge state of the polymer chain, thus enabling charge storage. Ions move towards the polymer backbone and undergo adsorption and desorption on or near the surface. This process is similar to the charge storage mechanism of capacitors but is referred to as pseudocapacitive behavior because it involves Faradaic reactions[145].

Fu et al.[146] successfully integrated polyaniline into lignin-based porous carbon through a one-step in-

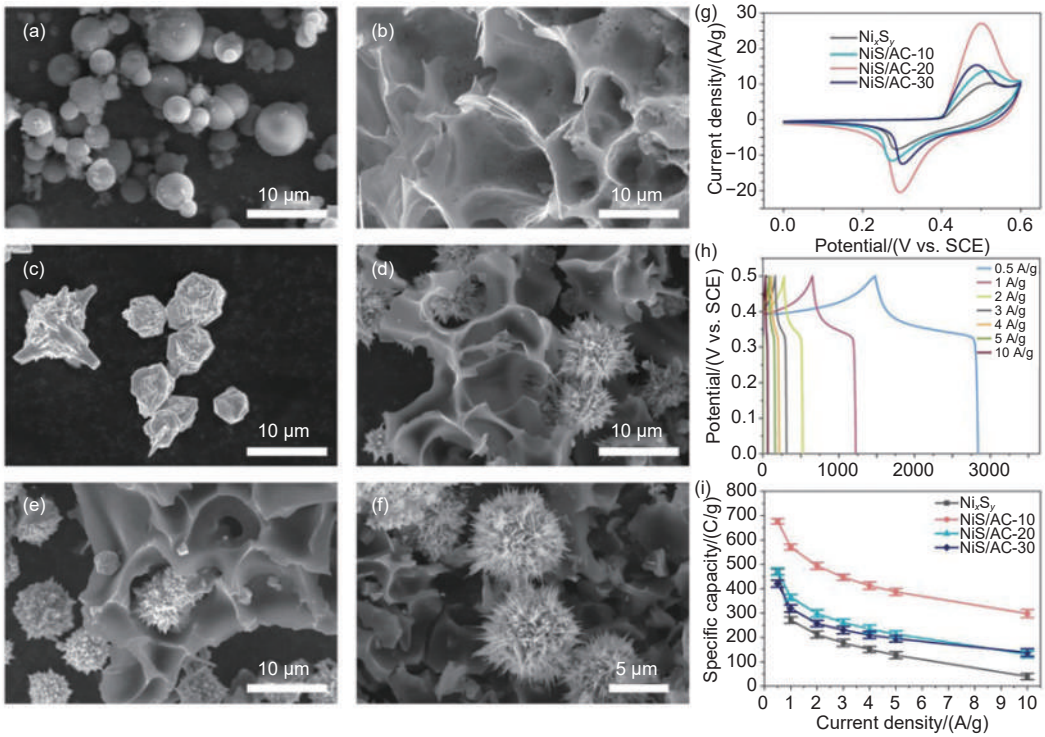

Fig. 13 SEM images of (a) lignin, (b) activated carbon (AC), (c)Ni_xS_y, (d-f) composite of NiS and AC with different ratios. (g) CV curves of Ni_xS_y and NiS/AC-10, 20, 30 at a scan rate of 5 mV s^{-1}. (h) Charge and discharge curves of NiS/AC-20 at different current densities. (i) The specific capacities of Ni_xS_y and NiS/AC-10, 20, 30 at different current densities. Adapted with permission from ref. [140]. Copyright 2022, Elsevier

situ polymerization process. They explored the compatibility of the lignin porous carbon with polyaniline and found that the lamellar hierarchical lignin porous carbon with crumpled nanosheets provided a large accessible SSA for the heterogeneous nucleation of aniline, ensuring a uniform loading of interpenetrating polyaniline nanofibers. This enhanced compatibility resulted in a composite with significantly improved electrochemical properties, showcasing a high capacitance of up to 643 F g^{-1} at 1.0 A g^{-1} and a substantial capacitance of 390 F g^{-1} at 30.0 A g^{-1}. According to Ehsani et al.[147], poly(o-aminophenol) (POAP) was loaded into the channel of lignin-based carbon, and POAP could be uniformly dispersed within the channel due to its high pore volume and surface area. When the specific capacity and retention rate of the initial capacity were examined, the results showed a high specific capacity of 485 F g^{-1} at a current density of 1.0 A g^{-1} and a good cycle stability of 86% after 3000 cycles.

Despite the promising properties of carbon-based conductive polymer composites, they encounter specific difficulties. It is challenging to establish effective and consistent adhesion between carbon materials and conductive polymers, regardless of whether the process involves physical mixing or chemical polymerization. Traditional preparation techniques often fail to create conductive polymer with ease, leading to the overabundance of branched polymer molecules or variations in the polymer layer's thickness[148]. Consequently, enhancing the composites' performance hinges on achieving a highly uniform interaction between different components and a controlled assembly of the conductive polymer's microstructure. Ruan et al.[148] suggested employing supercritical fluid technology in the synthesis process, which efficiently addresses the interface compatibility between the composites and markedly improves the electrochemical performance of the composite electrode materials. This research offers valuable insights into the integrated design of composites that boast enhanced electrochemical performance and improved interface compatibility.

For biomass-derived carbon-based composites,

researchers seem to have primarily focused on utilizing different metal oxides. Although some achievements have been made, the entire field still lacks universal interface regulation methods and exploration of the electron transport mechanism at the interface of composite materials.

4 Summary and outlook

In summary, lignin has the advantages of low cost, green and sustainable development, which gives great potential in producing porous carbon. And lignin-derived porous carbon with excellent electrochemical properties can be obtained through the selection of raw materials, optimization of preparation process and modification of products. By controlling these, lignin-based carbon can be used as a promising material for supercapacitor electrodes. This paper reviews the preparation process, activation mechanism and research progress of lignin-derived porous carbon in recent years, and discusses the effects of pore structure, heteroatoms, composites and other factors on its properties. And after decades of rapid development of high-density energy storage devices and miniaturization of electronic devices, supercapacitors remain of great significance for energy storage in a short time. Therefore, for a long time in the future, the development of lignin-based carbon or composites with low cost and high electrochemical performance for supercapacitor electrodes is highly promising.

Although lignin-based porous carbon has the above advantages, there are still many problems that need to be solved urgently in the commercial production of lignin based porous carbon: (1) Lignin obtained from different plant species usually has various morphologies, so the porous carbon will exhibit some differences in structure and surface properties. This is not limited to lignin, almost all biomass-derived carbon production is facing this problem. Therefore, it is necessary to develop promising pretreatment methods such as the hydrothermal method to obtain porous carbon with relatively regular morphology, for example, developing new hydrothermal additives. (2) There is relatively little research on the mechanism of pseudocapacitance caused by heteroatoms during the charging and discharging process, which directly hinders the design of heteroatom-doped carbon with better electrochemical performance. Especially now, the synergistic mechanism of polyatomic co-doping, the existence form and transformation mechanism of heteroatoms in the reaction are still unclear. Due to the development of in-situ electrochemical characterization technology, the future should focus on the transformation mechanism of heteroatoms in the charging and discharging process. (3) Although lignin is rich in functional groups, it can introduce various heteroatoms to promote the absorption and redox activity of electrodes. However, during the carbonization process, a large number of heteroatoms are lost, what's worse, the diversity of oxygenated functional groups results in different percentages of oxygen lost. So it's difficult for researchers to quantitatively regulate the amount of heteroatoms in lignin-based carbon. In order to optimize the heteroatom loss in the carbonization and improve the storage capacity and stability of supercapacitors, it is necessary to study more advanced carbonization technology (such as microwave-assisted carbonization, hydrothermal carbonization, laser carbonization) as well as more effective heteroatom protection technology. (4) For the activation method, the effect of physical activation is not good and the chemical activation requires high corrosion resistance of production equipment at high temperatures, due to the activation agents such as KOH, $ZnCl_2$, H_3PO_4. This is also the main problem encountered in the industrial production of lignin-based porous carbon. As for the template method, the pore size of lignin based porous carbon is relatively single due to the characteristics of hard template agents, while the soft template has limited effect on the regulation of the pore structure of lignin-based porous carbon. Therefore, it is necessary to develop novel, efficient and green activator and explore multifunctional and multiple template systems. (5) We need to construct a reasonable hierarchical interconnected pore structure, which further optimizes the ion transport kinetics, increases the effective contact area between the electrolyte and lignin-based porous carbon, shortens the

charge migration path, and provides a fast transfer path. On this basis, it is essential to establish the correlations between carbonization parameters and the resulting pore structure, crystalline structure, and surface characteristics of lignin-derived porous carbon. This understanding will be instrumental in guiding the large-scale manufacturing of functional lignin-based porous carbon.

Declaration of competing interest

The authors declare that they have no known competing financial interests or personal relationships that could have appeared to influence the work reported in this paper.

Acknowledgements

We gratefully acknowledgment the National Natural Science Foundation of China (22262034).

References

[1] Poonam, Sharma K, Arora A, et al. Review of supercapacitors: Materials and devices[J]. Journal of Energy Storage, 2019, 21: 801-825.

[2] Satpathy S, Das S, Bhattacharyya B K. How and where to use super-capacitors effectively, an integration of review of past and new characterization works on super-capacitors[J]. Journal of Energy Storage, 2020, 27: 101044.

[3] Li J L, Fleetwood J, Hawley W B, et al. From materials to cell: State-of-the-art and prospective technologies for lithium-ion battery electrode processing[J]. Chemical Reviews, 2022, 122(1): 903-956.

[4] Xie L J, Tang C, Song M X, et al. Molecular-scale controllable conversion of biopolymers into hard carbons towards lithium and sodium ion batteries: A review[J]. Journal of Energy Chemistry, 2022, 72: 554-569.

[5] Deng J, Luo W B, Chou S L, et al. Sodium-ion batteries: From academic research to practical commercialization[J]. Advanced Energy Materials, 2018, 8(4): 1701428.

[6] Zhang C, Wang S, Yang T, et al. Lithium superoxide-based high rate Li-Air batteries enabled by Di-iridium sulfur bridge active sites[J]. Energy Storage Materials, 2023, 60: 102844.

[7] Yaqoob L, Noor T, Iqbal N. An overview of metal-air batteries, current progress, and future perspectives[J]. Journal of Energy Storage, 2022, 56: 106075.

[8] Yadlapalli R T, Alla R R, Kandipati R, et al. Super capacitors for energy storage: Progress, applications and challenges[J]. Journal of Energy Storage, 2022, 49: 104194.

[9] Luo L, Lan Y, Zhang Q, et al. A review on biomass-derived activated carbon as electrode materials for energy storage supercapacitors[J]. Journal of Energy Storage, 2022, 55: 105839.

[10] Cao Q, Zhang Y, Chen J, et al. Electrospun biomass based carbon nanofibers as high-performance supercapacitors[J]. Industrial Crops and Products, 2020, 148: 112181.

[11] García-Mateos F J, Ruiz-Rosas R, María Rosas J, et al. Activation of electrospun lignin-based carbon fibers and their performance as self-standing supercapacitor electrodes[J]. Separation and Purification Technology, 2020, 241: 116724.

[12] Zeng Y, Zhang F, Wu J, et al. Green pepper-derived hierarchical porous carbon for supercapacitors with high performance[J]. Materials Advances, 2023, 4(9): 2192-2200.

[13] Simon P, Gogotsi Y. Materials for electrochemical capacitors[J]. Nature Materials, 2008, 7(11): 845-854.

[14] Chen R, Tang H, He P, et al. Interface engineering of biomass-derived carbon used as ultrahigh-energy-density and practical mass-loading supercapacitor electrodes[J]. Advanced Functional Materials, 2022, 33(8): 2212078.

[15] Chatterjee S, Saito T. Lignin-derived advanced carbon materials[J]. ChemSusChem, 2015, 8(23): 3941-3958.

[16] Upton B M, Kasko A M. Strategies for the conversion of lignin to high-value polymeric materials: Review and perspective[J]. Chemical Reviews, 2016, 116(4): 2275-2306.

[17] Lu Y, Wei X Y, Cao J P, et al. Characterization of a bio-oil from pyrolysis of rice husk by detailed compositional analysis and structural investigation of lignin[J]. Bioresource Technology, 2012, 116: 114-119.

[18] Nakashima J, Chen F, Jackson L, et al. Multi-site genetic modification of monolignol biosynthesis in alfalfa (Medicago sativa): effects on lignin composition in specific cell types[J]. New Phytologist, 2008, 179(3): 738-750.

[19] Davison B H, Drescher S R, Tuskan G A, et al. Variation of S/G ratio and lignin content in a populus family influences the release of xylose by dilute acid hydrolysis[J]. Applied Biochemistry and Biotechnology, 2006, 130(1): 427-435.

[20] Jakab E, Faix O, Till F. Thermal decomposition of milled wood lignins studied by thermogravimetry/mass spectrometry[J]. Journal of Analytical and Applied Pyrolysis, 1997, 40-41: 171-186.

[21] El Hage R, Brosse N, Chrusciel L, et al. Characterization of milled wood lignin and ethanol organosolv lignin from miscanthus[J].

Polymer Degradation and Stability, 2009, 94(10): 1632-1638.
[22] Wang J, Zhang M, Chen M, et al. Catalytic effects of six inorganic compounds on pyrolysis of three kinds of biomass[J]. Thermochimica Acta, 2006, 444(1): 110-114.
[23] Kim J Y, Oh S, Hwang H, et al. Structural features and thermal degradation properties of various lignin macromolecules obtained from poplar wood (Populus albaglandulosa)[J]. Polymer Degradation and Stability, 2013, 98(9): 1671-1678.
[24] Pan X, Kadla J F, Ehara K, et al. Organosolv ethanol lignin from hybrid poplar as a radical scavenger: relationship between lignin structure, extraction conditions, and antioxidant activity[J]. Journal of Agricultural and Food Chemistry, 2006, 54(16): 5806-5813.
[25] Chen L, Wang X, Yang H, et al. Study on pyrolysis behaviors of non-woody lignins with TG-FTIR and Py-GC/MS[J]. Journal of Analytical and Applied Pyrolysis, 2015, 113: 499-507.
[26] Wang S, Ru B, Lin H, et al. Pyrolysis behaviors of four lignin polymers isolated from the same pine wood[J]. Bioresource Technology, 2015, 182: 120-127.
[27] Liao Z, Zhu Y H, Sun G T, et al. Micromorphology control of the lignin-based activated carbon and the study on the pyrolysis and adsorption kinetics[J]. Industrial Crops and Products, 2022, 175: 114266.
[28] Singh K, Baheti V. A comprehensive review on activated carbon fabrics: preparation, characterization, and applications in electromagnetic interference shielding and joule heating[J]. Journal of Analytical and Applied Pyrolysis, 2024, 182: 106689.
[29] Yu B, Chang Z, Wang C. The key pre-pyrolysis in lignin-based activated carbon preparation for high performance supercapacitors[J]. Materials Chemistry and Physics, 2016, 181: 187-193.
[30] Shao S, Sun T, Li X, et al. Preparation of heavy bio-oil-based porous carbon by pyrolysis gas activation and its performance in the aldol condensation for aviation fuel as catalyst carrier[J]. Industrial Crops and Products, 2024, 218: 118963.
[31] Zeng F, Zhang Y, Lv Q, et al. Preparation of hierarchical porous carbon materials from bamboo shoot shells via air activation for high–performance supercapacitors[J]. International Journal of Electrochemical Science, 2024, 19(8): 100691.
[32] Fu K, Yue Q, Gao B, et al. Preparation, characterization and application of lignin-based activated carbon from black liquor lignin by steam activation[J]. Chemical Engineering Journal, 2013, 228: 1074-1082.
[33] Bergna D, Varila T, Romar H, et al. Activated carbon from hydrolysis lignin: Effect of activation method on carbon properties[J]. Biomass and Bioenergy, 2022, 159: 106387.
[34] Pakkang N, Kumar M, Taira S, et al. Preparation of kraft lignin-based activated carbon fiber electrodes for electric double layer capacitors using an ionic liquid electrolyte[J]. Holzforschung, 2020, 74(6): 577-588.
[35] Carrott P J M, Suhas, Carrott M M L R, et al. Reactivity and porosity development during pyrolysis and physical activation in CO_2 or steam of kraft and hydrolytic lignins[J]. Journal of Analytical and Applied Pyrolysis, 2008, 82(2): 264-271.
[36] Jiang Y, Ming C, Zhang S, et al. Activation of lignin-derived biochar with mixed H_2O and CO_2: Characterization of reaction intermediates and investigation their potential synergistic effects[J]. Journal of Analytical and Applied Pyrolysis, 2023, 176: 106242.
[37] Martínez-Alvarenga H, Gutiérrez M C, Benítez A, et al. Comprehensive study of valorisation of exhausted olive pomace through the preparation of highly porous activated carbons[J]. Fuel, 2024, 374: 132502.
[38] Islam M A, Nazal M K, Akinpelu A A, et al. Novel activated carbon derived from a sustainable and low-cost palm leaves biomass waste for tetracycline removal: Adsorbent preparation, adsorption mechanisms and real application[J]. Diamond and Related Materials, 2024, 147: 111375.
[39] Kumaravel S, Geetha M, Niyitanga T, et al. Preparation and characterization of activated carbon from corn cob by chemical activation and their adsorption of brilliant green dye from wastewater[J]. Process Safety and Environmental Protection, 2024, 188: 1338-1345.
[40] Fang Y Y, Zhang Q Y, Zhang D D, et al. The synthesis of porous carbons from a lignin-rich residue for high-performance supercapacitors[J]. New Carbon Materials, 2022, 37(4): 743-751.
[41] Liu S, Wei W G, Wu S B, et al. Efficient dichloromethane and toluene removal via lignin derived oxygen and nitrogen-containing activated carbons with well-developed micro-mesopore structure[J]. Diamond and Related Materials, 2022, 124: 108922.
[42] Yang Z, Gleisner R, H. Mann D, et al. Lignin based activated carbon using H_3PO_4 activation[J]. Polymers, 2020, 12(12): 2829.
[43] Wan X, Shen F, Hu J, et al. 3-D hierarchical porous carbon from oxidized lignin by one-step activation for high-performance supercapacitor[J]. International Journal of Biological Macromolecules, 2021, 180: 51-60.
[44] Yin J, Zhang W, Alhebshi N A, et al. Synthesis strategies of porous carbon for supercapacitor applications[J]. Small Methods, 2020, 4(3): 1900853.
[45] Yorgun S, Vural N, Demiral H. Preparation of high-surface area activated carbons from Paulownia wood by $ZnCl_2$ activation[J]. Microporous and Mesoporous Materials, 2009, 122(1): 189-194.
[46] Hu J, Shen D, Wu S, et al. Insight into the effect of $ZnCl_2$ on analytical pyrolysis behavior of cellulolytic enzyme corn stover lignin[J]. Journal of Analytical and Applied Pyrolysis, 2017, 127: 444-450.
[47] Zhao J, Zhang W, Shen D, et al. Preparation of porous carbon materials from black liquor lignin and its utilization as CO_2 adsorbents[J]. Journal of the Energy Institute, 2023, 107: 101179.
[48] Wu Y, Cao J P, Hao Z Q, et al. One-step preparation of alkaline lignin-based activated carbons with different activating agents for electric double layer capacitor[J]. International Journal of Electrochemical Science, 2017, 12(8): 7227-7239.
[49] Li X, Wang B, Lu F, et al. A one-stone-two-birds strategy to lignin-derived porous carbon for supercapacitor electrodes[J]. Diamond and Related Materials, 2024, 142: 110831.
[50] Yan L, Liu A, Ma R, et al. Regulating the specific surface area and

porous structure of carbon for high performance supercapacitors[J]. Applied Surface Science, 2023, 615: 156267.

[51] Albadarin A B, Al-Muhtaseb A a H, Walker G M, et al. Retention of toxic chromium from aqueous phase by H_3PO_4-activated lignin: Effect of salts and desorption studies[J]. Desalination, 2011, 274(1): 64-73.

[52] Yang H, Chen P, Chen W, et al. Insight into the formation mechanism of N, P co-doped mesoporous biochar from H_3PO_4 activation and NH_3 modification of biomass[J]. Fuel Processing Technology, 2022, 230: 107215.

[53] Li H, Zhao Y, Liu S, et al. Hierarchical porous carbon monolith derived from lignin for high areal capacitance supercapacitors[J]. Microporous and Mesoporous Materials, 2020, 297: 109960.

[54] Zhao X, Gao P, Shen B, et al. Recent advances in lignin-derived mesoporous carbon based-on template methods[J]. Renewable and Sustainable Energy Reviews, 2023, 188: 113808.

[55] Wu K J, Yang C Y, Liu Y, et al. Hierarchical meso- and macroporous carbon from lignin for kraft lignin decomposition to aromatic monomers[J]. Catalysis Today, 2021, 365: 214-222.

[56] Dhumal N R, Gejji S P. Theoretical studies in local coordination and vibrational spectra of $M^+CH_3O(CH_2CH_2O)_nCH_3$ (n=2–7) complexes (M=Na, K, Mg and Ca)[J]. Chemical Physics, 2006, 323(2): 595-605.

[57] Song Y G, Liu J L, Sun K, et al. Synthesis of sustainable lignin-derived mesoporous carbon for supercapacitors using a nano-sized MgO template coupled with Pluronic F127[J]. RSC Advances, 2017, 7(76): 48324-48332.

[58] Peng L, Hung C T, Wang S, et al. Versatile nanoemulsion assembly approach to synthesize functional mesoporous carbon nanospheres with tunable pore sizes and architectures[J]. Journal of the American Chemical Society, 2019, 141(17): 7073-7080.

[59] Seo J, Park H, Shin K, et al. Lignin-derived macroporous carbon foams prepared by using poly(methyl methacrylate) particles as the template[J]. Carbon, 2014, 76: 357-367.

[60] Qin H, Jian R, Bai J, et al. Influence of molecular weight on structure and catalytic characteristics of ordered mesoporous carbon derived from lignin[J]. ACS Omega, 2018, 3(1): 1350-1356.

[61] Wang N, Hu Y, Ke X, et al. Enhanced-absorption template method for preparation of double-shell NiO hollow nanospheres with controllable particle size for nanothermite application[J]. Chemical Engineering Journal, 2020, 379: 122330.

[62] Saini K, Sahoo A, Biswas B, et al. Preparation and characterization of lignin-derived hard templated carbon(s): Statistical optimization and methyl orange adsorption isotherm studies[J]. Bioresource Technology, 2021, 342: 125924.

[63] Zhang B, Yang D, Qiu X, et al. Fabricating ZnO/lignin-derived flower-like carbon composite with excellent photocatalytic activity and recyclability[J]. Carbon, 2020, 162: 256-266.

[64] wang X, Li X, Lu Z, et al. Constructing porous lignin-based carbon nanofiber anodes with flexibility for high-performance lithium/sodium-ion batteries[J]. Materials Today Sustainability, 2022, 20: 100234.

[65] Wang S, Feng J, Pan H. Facile preparation of nitrogen-doped hierarchical porous carbon derived from lignin with KCl for supercapacitors[J]. Colloids and Surfaces A: Physicochemical and Engineering Aspects, 2022, 651: 129622.

[66] Xie A T, Dai J D, Chen Y, et al. NaCl-template assisted preparation of porous carbon nanosheets started from lignin for efficient removal of tetracycline[J]. Advanced Powder Technology, 2019, 30(1): 170-179.

[67] Wu K, Liu Y, Yang C, et al. Tuning the mesopore size of lignin-based porous carbon via salt templating for kraft lignin decomposition[J]. Industrial Crops and Products, 2022, 181: 114865.

[68] Zhou G, Jia X, Zhang X, et al. Multi-walled carbon nanotube-modified hydrothermal carbon: A potent carbon material for efficient remediation of cadmium-contaminated soil in coal gangue piling site[J]. Chemosphere, 2022, 307: 135605.

[69] Teng Y, Li W, Wang J, et al. A green hydrothermal synthesis of polyacrylonitrile@carbon/MIL-101(Fe) composite nanofiber membrane for efficient selective removal of tetracycline[J]. Separation and Purification Technology, 2023, 315: 123610.

[70] Lv Y, Xue J, Chen Z, et al. Development of hydrothermal carbonaceous carbon/NH_2-MIL-101(Fe) composite photocatalyst with in-situ production and activation of H_2O_2 capabilities for effective sterilization[J]. Chemical Engineering Journal, 2024, 498: 155263.

[71] Guo Q, Qiao S, Zhang D, et al. A comparison of hydrothermal carbonization versus pyrolysis-activation for sludge-derived carbon materials on physiochemical properties and electrochemical performance[J]. Biomass and Bioenergy, 2024, 182: 107079.

[72] Kim D, Lee K, Park K Y. Upgrading the characteristics of biochar from cellulose, lignin, and xylan for solid biofuel production from biomass by hydrothermal carbonization[J]. Journal of Industrial and Engineering Chemistry, 2016, 42: 95-100.

[73] Wang C, Zhang S, Wu S, et al. Multi-purpose production with valorization of wood vinegar and briquette fuels from wood sawdust by hydrothermal process[J]. Fuel, 2020, 282: 118775.

[74] Gao Q, Titirici M M. Achieving high volumetric EDLC carbons via hydrothermal carbonization and cyclic activation[J]. Journal of Physics: Energy, 2020, 2(2): 025005.

[75] Li H, Shi F, An Q, et al. Three-dimensional hierarchical porous carbon derived from lignin for supercapacitors: Insight into the hydrothermal carbonization and activation[J]. International Journal of Biological Macromolecules, 2021, 166: 923-933.

[76] Jain K, Singh M, Yadav K, et al. Direct conversion of lignin-rich black liquor to activated carbon for supercapacitor electrodes[J]. International Journal of Biological Macromolecules, 2024, 270: 132150.

[77] Wang H, Xiong F, Guo F, et al. Constructing monodisperse blueberry-like lignin-based porous carbon nanospheres for high-performance supercapacitors[J]. Colloids and Surfaces A: Physicochemical and Engineering Aspects, 2022, 655: 130237.

[78] Lynam J G, Toufiq Reza M, Vasquez V R, et al. Effect of salt

addition on hydrothermal carbonization of lignocellulosic biomass[J]. Fuel, 2012, 99: 271-273.

[79] Hasan R O, Ercan B, Acikkapi A N, et al. Effects of metal chlorides on the hydrothermal carbonization of grape seeds[J]. Energy & Fuels, 2021, 35(10): 8834-8843.

[80] Wu Y, Cao J P, Zhao X Y, et al. High-performance electrode material for electric double-layer capacitor based on hydrothermal pre-treatment of lignin by $ZnCl_2$[J]. Applied Surface Science, 2020, 508: 144536.

[81] Chmiola J, Yushin G, Gogotsi Y, et al. Anomalous increase in carbon capacitance at pore sizes less than 1 nanometer[J]. Science, 2006, 313(5794): 1760-1763.

[82] Huang J, Sumpter B G, Meunier V. A universal model for nanoporous carbon supercapacitors applicable to diverse pore regimes, carbon materials, and electrolytes[J]. Chemistry – A European Journal, 2008, 14(22): 6614-6626.

[83] Huang J, Sumpter B G, Meunier V. Theoretical model for nanoporous carbon supercapacitors[J]. Angewandte Chemie International Edition, 2008, 47(3): 520-524.

[84] Girirajan M, Bojarajan A K, Pulidindi I N, et al. An insight into the nanoarchitecture of electrode materials on the performance of supercapacitors[J]. Coordination Chemistry Reviews, 2024, 518: 216080.

[85] Huang T, Wen F, Zheng Y, et al. Building mesoporous channels in lignin-derived microporous carbons to remold the electrochemical behaviors of supercapacitors[J]. Journal of Power Sources, 2024, 621: 235328.

[86] Guo S, Li H, Zhang X, et al. Lignin carbon aerogel/nickel binary network for cubic supercapacitor electrodes with ultra-high areal capacitance[J]. Carbon, 2021, 174: 500-508.

[87] Han F, Jing W, Wu Q, et al. Nitrogen-doped graphene fiber electrodes with optimal micro-/meso-/macro-porosity ratios for high-performance flexible supercapacitors[J]. Journal of Power Sources, 2022, 520: 230866.

[88] Zhao L, Jian W, Zhang X, et al. Multi-scale self-templating synthesis strategy of lignin-derived hierarchical porous carbons toward high-performance zinc ion hybrid supercapacitors[J]. Journal of Energy Storage, 2022, 53: 105095.

[89] Levi M D, Salitra G, Levy N, et al. Application of a quartz-crystal microbalance to measure ionic fluxes in microporous carbons for energy storage[J]. Nature Materials, 2009, 8(11): 872-875.

[90] Forse A C, Griffin J M, Wang H, et al. Nuclear magnetic resonance study of ion adsorption on microporous carbide-derived carbon[J]. Physical Chemistry Chemical Physics, 2013, 15(20): 7722-7730.

[91] Kruusma J, Tõnisoo A, Pärna R, et al. In situ XPS studies of electrochemically positively polarized molybdenum carbide derived carbon double layer capacitor electrode[J]. Journal of the Electrochemical Society, 2014, 161(9): A1266.

[92] Tõnisoo A, Kruusma J, Pärna R, et al. In situ XPS studies of electrochemically negatively polarized molybdenum carbide derived carbon double layer capacitor electrode[J]. Journal of the Electrochemical Society, 2013, 160(8): A1084.

[93] Chen J, Rao X, Zhang F, et al. Unveiling activated carbon degradation in supercapacitor using liquid cell transmission electron microscopy[J]. ACS Applied Energy Materials, 2024, 7(21): 9797-9805.

[94] Taslim R, Refanza R, Hamdy M I, et al. One-step strategy of 3D hierarchical porous carbon with self-heteroatom-doped derived bread waste for high-performance supercapacitor[J]. Journal of Analytical and Applied Pyrolysis, 2023, 171: 105956.

[95] Zhang Y, Wu C, Dai S, et al. Rationally tuning ratio of micro- to meso-pores of biomass-derived ultrathin carbon sheets toward supercapacitors with high energy and high power density[J]. Journal of Colloid and Interface Science, 2022, 606: 817-825.

[96] Li D, Huang Y, Yu C, et al. Pore structure regulation of hierarchical porous agaric-derived carbon via boric acid activation for supercapacitors[J]. Diamond and Related Materials, 2022, 130: 109432.

[97] Zhu J, Huang T, Lu M, et al. Sustainable lignin-derived hierarchical mesoporous carbon synthesized by a renewable nano-calcium carbonate hard template method and its utilization in zinc ion hybrid supercapacitors[J]. Green Chemistry, 2024, 26(9): 5441-5451.

[98] Ma C, Song G, Li Z, et al. High-areal-capacitance electrode constructed by lignin-based microporous carbon nanofibers for supercapacitors[J]. Journal of Energy Storage, 2024, 88: 111465.

[99] Cao Q, Zhu H, Xu J, et al. Research progress in the preparation of lignin-based carbon nanofibers for supercapacitors using electrospinning technology: A review[J]. International Journal of Biological Macromolecules, 2024, 273: 133037.

[100] Du B, Zhu H, Chai L, et al. Effect of lignin structure in different biomass resources on the performance of lignin-based carbon nanofibers as supercapacitor electrode[J]. Industrial Crops and Products, 2021, 170: 113745.

[101] Song M, Yu L, Song B, et al. Alkali promoted the adsorption of toluene by adjusting the surface properties of lignin-derived carbon fibers[J]. Environ Sci Pollut Res Int, 2019, 26(22): 22284-22294.

[102] Xu D, Xuan D, Liao Y, et al. Lignin-derived carbon membrane for the preparation of composite electrodes and applications in supercapacitors[J]. Diamond and Related Materials, 2022, 129: 109344.

[103] Bai Q, Zhang G, Bai X, et al. The design of binder-free self-supporting carbon paper electrode based on biomass derived hierarchical porous carbon/cellulose nanofibers for sustainable flexible supercapacitors[J]. Applied Surface Science, 2024, 678: 161140.

[104] Yang Z, Tang K, Song W, et al. Coaxial direct writing of ultra-strong supercapacitors with braided continuous carbon fiber based electrodes[J]. Chemical Engineering Journal, 2024, 499: 155875.

[105] Wang H, Xiong F, Yang J, et al. Preparation of size-controlled all-lignin based carbon nanospheres and their electrochemical performance in supercapacitor[J]. Industrial Crops and Products, 2022, 179: 114689.

[106] Wang T, Liu Z, Li P, et al. Lignin-derived carbon aerogels with

high surface area for supercapacitor applications[J]. Chemical Engineering Journal, 2023, 466: 143118.

[107] Feng S, Fan Q, Ouyang Q, et al. Morphology and structure control of lignin-derived hierarchical porous carbon for high-performance supercapacitors[J]. Colloids and Surfaces A: Physicochemical and Engineering Aspects, 2024, 685: 133292.

[108] Li W, Zhang W, Xu Y, et al. Heteroatom-doped lignin derived carbon materials with improved electrochemical performance for advanced supercapacitors[J]. Chemical Engineering Journal, 2024, 497: 154829.

[109] Gao Y, Zhang J, Luo X, et al. Energy density-enhancement mechanism and design principles for heteroatom-doped carbon supercapacitors[J]. Nano Energy, 2020, 72: https://doi.org/10.1016/j.nanoen.2020.104666.

[110] Sharma K, Kadyan P, Sharma R K, et al. Heteroatom doping in bio-waste derived activated carbon for enhanced supercapacitor performance: A review[J]. Journal of Energy Storage, 2024, 100: 113679.

[111] Dong D, Zhang Y, Xiao Y, et al. High performance aqueous supercapacitor based on nitrogen-doped coal-based activated carbon electrode materials[J]. Journal of Colloid and Interface Science, 2020, 580: 77-87.

[112] Xu S W, Dai J X, Wang M D, et al. Role of Nitrogen-doping in porous carbon for enlarging working voltage window of aqueous supercapacitors in neutral electrolyte[J]. Chemical Engineering Journal, 2024, 499: 155880.

[113] Duignan T T, Zhao X S. Impurities limit the capacitance of carbon-based supercapacitors[J]. The Journal of Physical Chemistry C, 2019, 123(7): 4085-4093.

[114] Yang J, Xiong F, Wang H, et al. Facile and scalable construction of nitrogen-doped lignin-based carbon nanospheres for high-performance supercapacitors[J]. Fuel, 2023, 343: 128007.

[115] Wen F, Yan Y, Sun S, et al. Synergistic effect of nitrogen and oxygen dopants in 3D hierarchical porous carbon cathodes for ultra-fast zinc ion hybrid supercapacitors[J]. Journal of Colloid and Interface Science, 2023, 640: 1029-1039.

[116] Ghosh S, Barg S, Jeong S M, et al. Heteroatom-doped and oxygen-functionalized nanocarbons for high-performance supercapacitors[J]. Advanced Energy Materials, 2020, 10(32): 2001239.

[117] Shaheen Shah S, Abu Nayem S M, Sultana N, et al. Preparation of sulfur-doped carbon for supercapacitor applications: A review[J]. ChemSusChem, 2022, 15(1): e202101282.

[118] Nankya R, Opar D O, Kim M J, et al. Synergetic effect of nitrogen and sulfur co-doping in mesoporous graphene for enhanced energy storage properties in supercapacitors and lithium-ion batteries[J]. Journal of Solid State Chemistry, 2020, 289: 121451.

[119] Chen L, Li X, Ma C, et al. Interaction and quantum capacitance of nitrogen/sulfur co-doped graphene: A theoretical calculation[J]. The Journal of Physical Chemistry C, 2017, 121(34): 18344-18350.

[120] Yin W M, Tian L F, Pang B, et al. Fabrication of dually N/S-doped carbon from biomass lignin: Porous architecture and high-rate performance as supercapacitor[J]. International Journal of Biological Macromolecules, 2020, 156: 988-996.

[121] Fan Y, Fu F, Yang D, et al. Thiocyanogen-modulated N, S Co-doped lignin hierarchical porous carbons for high-performance aqueous supercapacitors[J]. Journal of Colloid and Interface Science, 2024, 667: 147-156.

[122] Shi F, Tong Y, Li H, et al. Synthesis of oxygen/nitrogen/sulfur codoped hierarchical porous carbon from enzymatically hydrolyzed lignin for high-performance supercapacitors[J]. Journal of Energy Storage, 2022, 52: 104992.

[123] Niu L, Li Z, Hong W, et al. Pyrolytic synthesis of boron-doped graphene and its application as electrode material for supercapacitors[J]. Electrochimica Acta, 2013, 108: 666-673.

[124] Poornima B H, Vijayakumar T. Hydrothermal synthesis of Boron - doped porous carbon from Azadirachta Indica wood for supercapacitor application[J]. Inorganic Chemistry Communications, 2022, 145: 109953.

[125] Paraknowitsch J P, Thomas A. Doping carbons beyond nitrogen: an overview of advanced heteroatom doped carbons with boron, sulphur and phosphorus for energy applications[J]. Energy & Environmental Science, 2013, 6(10): 2839-2855.

[126] Luo L, Zhou Y L, Yan W, et al. Two-step synthesis of B and N co-doped porous carbon composites by microwave-assisted hydrothermal and pyrolysis process for supercapacitor application[J]. Electrochimica Acta, 2020, 360: 137010.

[127] Roberts V M, Stein V, Reiner T, et al. Towards quantitative catalytic lignin depolymerization[J]. Chemistry – A European Journal, 2011, 17(21): 5939-5948.

[128] Dong Z, Yang H, Liu Z, et al. Pyrolysis of boron-crosslinked lignin: Influence on lignin softening and product properties[J]. Bioresource Technology, 2022, 355: 127218.

[129] Dong Z, Yang H, Liu Z, et al. Effect of boron-based additives on char agglomeration and boron doped carbon microspheres structure from lignin pyrolysis[J]. Fuel, 2021, 303: 121237.

[130] Saha U, Jaiswal R, Goswami T H, et al. Cobalt ferrite ($CoFe_2O_4$)–activated carbon fabric (ACF) based composite electrode material for supercapacitor application[J]. Journal of Energy Storage, 2024, 99: 113218.

[131] Li R, Lu Y, Lyu X, et al. A comprehensive study on two types of supercapacitor composite electrodes comprising MnO_2 and activated carbon nanofibers: Self-supporting membrane and ground powder[J]. Journal of Energy Storage, 2024, 92: 112196.

[132] Chen M, Zeng T, Luo L, et al. Binary transition metal sulfides MoS_2–NiS_2 anchored on biomass-derived carbon for improved performance of lithium–sulfur batteries[J]. Journal of Alloys and Compounds, 2024, 984: 173969.

[133] Ullah S, Rehman A u, Najam T, et al. Advances in metal-organic framework@activated carbon (MOF@AC) composite materials: Synthesis, characteristics and applications[J]. Journal of Industrial and Engineering Chemistry, 2024, 137: 87-105.

[134] Sui S, Sha J, Deng X, et al. Boosting the charge transfer efficiency of metal oxides/carbon nanotubes composites through interfaces control[J]. Journal of Power Sources, 2021, 489: 229501.

[135] Shi F, Li J, Xiao J, et al. Three-dimensional hierarchical porous lignin-derived carbon/WO_3 for high-performance solid-state planar micro-supercapacitor[J]. International Journal of Biological Macromolecules, 2021, 190: 11-18.

[136] Mu J, Li C, Zhang J, et al. Efficient conversion of lignin waste and self-assembly synthesis of C@$MnCo_2O_4$ for asymmetric supercapacitors with high energy density[J]. Green Energy & Environment, 2022, 8(5): 1479-1487.

[137] Dai Z, Zhang Y, Ma Y, et al. Nickel-cobalt-TiO_2 co-doped lignin based carbon nanofibers: Versatile integrated material for supercapacitor and microwave absorption[J]. Diamond and Related Materials, 2023, 139: 110330.

[138] Abdel Maksoud M I A, Fahim R A, Shalan A E, et al. Advanced materials and technologies for supercapacitors used in energy conversion and storage: a review[J]. Environmental Chemistry Letters, 2021, 19(1): 375-439.

[139] Cui M, Meng X. Overview of transition metal-based composite materials for supercapacitor electrodes[J]. Nanoscale Advances, 2020, 2(12): 5516-5528.

[140] Cao S, Li H, Zhou X, et al. NiS/activated carbon composite derived from sodium lignosulfonate for long cycle-life asymmetric supercapacitors[J]. Journal of Alloys and Compounds, 2022, 900: 163546.

[141] Li J, Yang J, Wang P, et al. $NiCo_2S_4$ combined 3D hierarchical porous carbon derived from lignin for high-performance supercapacitors[J]. International Journal of Biological Macromolecules, 2023, 232: 123344.

[142] Kayode S E, Sánchez-Rodríguez C E, López-Sandoval R, et al. Oxidative calcination of brewery bagasse and in-situ preparation of activated carbon-PEDOT composite for hybrid supercapacitor application[J]. Synthetic Metals, 2024, 309: 117735.

[143] Gmucová K. Fundamental aspects of organic conductive polymers as electrodes[J]. Current Opinion in Electrochemistry, 2022, 36: 101117.

[144] Loganathan N N, Perumal V, Pandian B R, et al. Recent studies on polymeric materials for supercapacitor development[J]. Journal of Energy Storage, 2022, 49: 104149.

[145] Saha S, Samanta P, Murmu N C, et al. A review on the heterostructure nanomaterials for supercapacitor application[J]. Journal of Energy Storage, 2018, 17: 181-202.

[146] Fu F, Wang H, Yang D, et al. Lamellar hierarchical lignin-derived porous carbon activating the capacitive property of polyaniline for high-performance supercapacitors[J]. Journal of Colloid and Interface Science, 2022, 617: 694-703.

[147] Ehsani A, Moftakhar M K, karimi F. Lignin-derived carbon as a high efficient active material for enhancing pseudocapacitance performance of p-type conductive polymer[J]. Journal of Energy Storage, 2021, 35: 102291.

[148] Ruan S, Xin W J, Wang C, et al. An approach to enhance carbon/polymer interface compatibility for lithium-ion supercapacitors[J]. Journal of Colloid and Interface Science, 2023, 652: 1063-1073.